Robust Consensus of High-Order Systems under Output Constraints: Application to Rendezvous of Underactuated UAVs

Esteban Restrepo, Antonio Loria, Ioannis Sarras, Julien Marzat

Robust Consensus of High-Order Systems under Output Constraints: Application to Rendezvous of Underactuated UAVs

Esteban Restrepo Antonio Loría Ioannis Sarras Julien Marzat

***Abstract*— We address the output and state consensus problems for multi-agent high-order systems in feedback form under realistic conditions. First, under the premise that measurements may be of different kinds, we consider systems interconnected over undirected-topology networks as well as directed spanning-trees and directed cycles. Second, we assume that the systems may be subject to multiple restrictions in the form of output or state constraints, such as limited-range measurements, physical limitations imposed by the actuators or by the environment, etc. In addition, we suppose that the systems may be subject to external disturbances, such as undesired forces or modeling uncertainties. Under these conditions, we provide a control framework and a formal analysis that establishes robust stability in the input-to-state sense. The former relies on a modified backstepping method and the latter on multi-stability theory. In addition, we show how our approach applies to meaningful problems of physical systems through a case-study of interest in the aerospace industry: safety-aware rendezvous control of underactuated UAVs subject to connectivity and collision-avoidance constraints.**

I. Introduction

A. Problem description

Consensus control constitutes the basis of cooperative interaction for multi-agent systems [1], [2]. For instance, in the case of (robotic) vehicles the consensus objective is fundamental to achieve complex formation *maneuvering* tasks [3]. Hence, the literature is rife with works addressing diverse consensus problems for a variety of dynamical systems, such as linear systems [4]–[6], relative-degree-one nonholonomic vehicles [7], or second-order Euler-Lagrange systems [8], [9], to mention a few. However, such models may fall short at representing many meaningful and complex engineering problems in which the input-output relationship imposes a high relative degree (with respect to an output of interest) model. Consensus of high-order systems has been addressed, for instance, in [10]–[13]. A good example of high-order systems is that of certain autonomous vehicles —see [1], [2], [14], and Section V in this paper.

E. Restrepo, I. Sarras, and J. Marzat are with DTIS, ONERA, Université Paris-Saclay, F-91123 Palaiseau, France. E-mail: {esteban.restrepo, ioannis.sarras, julien.marzat}@onera.fr. A. Loría is with L2S, CNRS, 91192 Gif-sur-Yvette, France. E-mail: aloria@ieee.org E. Restrepo is also with L2S-CentraleSupélec, Université Paris-Saclay, Saclay, France. The work of A. Loría was supported by the French ANR via project HANDY, contract number ANR-18-CE40-0010 and by CEFIPRA under the grant number 6001-A.

On the other hand, in realistic settings, physical systems operate under multiple restrictions in the form of output or state constraints such as limited range measurements/communication, physical limitations imposed by the actuators (input saturation) or the environment (collisions, bounded workspace). In addition, such systems are constantly subject to disturbances such as external inputs, modeling uncertainties, delays, etc. Thus, for consensus control laws to be of practical use, constraints must be considered and robustness with respect to disturbances must be guaranteed. These pose significant challenges for control design and formal analysis that we address in this paper.

A good example of a scenario of cooperative systems in which a plethora of difficulties appear naturally is that of rendezvous control of unmanned-autonomous vehicles (UAVs). First, the systems' dynamics are clearly nonlinear and underactuated [15]. Therefore, the literature on consensus tailored for linear low-order systems [1], [16] does not apply. Second, the measurements usually come from embedded relative-measurement sensors, such as cameras, LiDAR, ultrasound, etc. The use of such devices naturally imposes directed network topologies [17], which add difficulty to the consensus-control design. Third, autonomous vehicles moving "freely" in the workspace are prone to undesired collisions among themselves; therefore, guaranteeing the safety of the system in the sense of inter-agent collision avoidance is a restriction that must be considered as well. A fourth difficulty stems from the use of on-board relative-measurement devices, which are reliable only if used within a limited range. This translates into guaranteeing that the UAVs do not drift "too far" apart from their neighbors. Finally, UAVs are constantly subject to external undesired forces and they may also be affected by modeling uncertainties, etc.; these constitute external disturbances at different levels in the dynamic model.

B. Literature review

The characteristics described above coin a realistic scenario of automatic control of multi-agent systems, not restricted to UAVs. Consensus under such conditions has been addressed in the literature, but to the best of our knowledge never simultaneously.

There are many articles that address the constrained consensus problem for low-order systems interconnected over, both, undirected and directed topologies [16], [18]–[21]. Fewer

works, however, address the consensus control problem with constraints for high-order systems. In [22] a *tracking* consensus controller is proposed for networked systems over undirected graphs, but the constraints are considered on the synchronization error and not directly on the inter-agent relative states. In [23] a synchronization control is designed using an adaptation of the prescribed performance framework in order to achieve consensus over directed graphs with desired bounds on the transient response. Nevertheless, as in [22], the prescribed-performance constraints are imposed on the consensus error and not on the inter-agent relative states. A consensus control for high-order systems with constraints and interacting over strongly connected directed graphs is presented in [24]. Yet, the constraints considered therein weigh on each individual agent's states (e.g., constraints on the velocity, the acceleration, etc.), and do not reflect inter-agent restrictions.

In the case of rendezvous of underactuated UAVs, only a handful of works in the literature consider the problem under a set of realistic assumptions while not at the expense of formal analysis. A distributed controller is proposed in [25] based on prescribed-performance control that achieves formation tracking with collision avoidance for multiple UAVs. Nonetheless, the results therein apply only to undirected topologies. Based on the attitude and thrust extraction algorithm, the authors in [26] solve the formation problem for multiple UAVs subject to connectivity constraints, but only undirected topologies are considered and collision-avoidance constraints are not addressed. In [8], [9], and [27] robust formation controllers are proposed based on the prescribed-performance-control [28] and edge-agreement frameworks [14], [29], guaranteeing, also, collision avoidance and connectivity maintenance. However, in these references only fully-actuated Lagrangian systems interconnected over undirected-tree topologies are considered.

C. This paper's contents in perspective

In this paper we propose a control method that applies to nonlinear systems in feedback form and covers, simultaneously, all aspects evoked above. The systems' model and the problem formulation are described in detail in Section II.

As the study of networked systems over undirected graphs is better covered by the literature, our main statements are formulated only for directed spanning trees and directed cycles. These directed topologies present practical interests of their own as they appear naturally in leader-follower configurations [1], [2] and in the context of cyclic pursuit [30]. Our control approach, however, also applies to systems interconnected over undirected graphs. To guarantee the systems' safety as well as the integrity of the topology through the maintenance of connectivity, our controllers guarantee that *output* constraints are respected. Essentially, these take the mathematical form of a lower and an upper bound on the norm of relative-error states, which are more natural inter-agent constraints than those considered, e.g., in [22] and [23]. Then, the said constraints are encoded in the control design via laws that are derived as the gradient of barrier Lyapunov functions [31]. Loosely speaking, the control may be assimilated to a force field that "explodes" near the limits to avoid. That is, the control input as a function of the state grows unboundedly as the vehicle approaches a specified region. This technique is also reminiscent of potential/navigation functions used in robot control [27], [32].

Now, because we consider systems in feedback form, the control design also appeals to the popular passivity-based *backstepping* method [33]. However, since in the presence of constraints this may involve successive derivatives of functions with multiple saddle points, we use the command-filtered backstepping approach [34], in which the successive derivatives are approximated by linear strictly-positive-real filters. We describe our control-design framework for systems in feedback form in Section III.

In regards to the formal analysis, it is important to stress that in contrast to the more-often used nodes-based graph modeling approach, our approach is based on the edge-agreement framework introduced in [29]. Since in this framework the consensus problem is recast as one of stabilization of the origin, it constitutes a more natural setting for the consideration of inter-agent constraints. Furthermore, since inter-agent constraints may introduce undesired unstable equilibria within the edges' perspective, the closed-loop system is analyzed relying on the theory of multi-stable systems [35], [36]. Based on the latter, we establish asymptotic convergence of the multi-agent system to the consensus manifold, as well as robustness with respect to external disturbances in the sense of practical-input-to-state stability. This property cannot be overestimated; it is stronger than mere convergence, which is more commonly established in the literature —see, e.g., [24], [37]– [39], [40]. Indeed, input-to-state stability implies boundedness of the systems' state trajectories and the satisfaction of the inter-agent output constraints may also be assessed, even in the presence of external disturbances. The same cannot be ascertained if in the absence of disturbances it is only known that the errors converge. We provide a formal analysis of our control approach in Section IV.

Beyond our main theoretical findings, in Section V we show how our framework may be applied to the rendezvous control problem for a group of underactuated UAVs, subject to connectivity and collision avoidance constraints, using only local information from its neighbors. This is a relevant problem to the aerospace industry that is motivated by the increasing interest for safety-aware fleet deployment. It is fitting to mention that similar problems have been studied in the literature, as for instance in [25], [26], but only for systems interconnected over undirected graphs. A more detailed description of this problem and of our contributions relative to the literature is presented in Section V as well.

The paper is wrapped up with some Concluding remarks in Section VI and complementary technical Appendices.

II. Model and problem formulation

We consider multi-agent nonlinear systems in feedback form with high relative degree with respect to an output of interest. Plants that fit in this category include fully feedback-linearizable systems, but also a number of instances of physical

systems, such as robot manipulators [41], flying vehicles [42], spacecrafts [43], flexible-joint manipulators [44], [45], etc.

Now, for simplicity and without loss of generality, in the following theoretical development we consider that each agent is modeled as a high-order system in normal form subject to additive disturbances. More precisely, we consider N multi-variable systems in normal form and of relative degree ρ as follows:

$$\dot{x}_{i,l} = x_{i,l+1} + \theta_{i,l}(t), \quad l \leq \rho - 1 \tag{1a}$$

$$\dot{x}_{i,\rho} = u_i + \theta_{i,\rho}(t) \tag{1b}$$

where $x_{i,l} \in \mathbb{R}^n$, $l \leq \rho$, $i \leq N$, denotes the components of the state of each agent, $u_i \in \mathbb{R}^n$ is the control input, $\theta_{i,l} : \mathbb{R}_{\geq 0} \mapsto \mathbb{R}^n$ is an essentially bounded function that represents a disturbance, and $x_{i,1}$ is considered an output of interest.

Note that many systems in feedback form can be transformed into (1) through different nonlinear control approaches, such as feedback linearization, input transformation, etc. [33], [46]. The systems (1) cover, for instance, second-order feedback linearizable systems in which the output-consensus problem consists in driving all the positions $x_{i,1}$ to a common constant value and all the velocities $x_{i,2}$ to zero. This problem has been studied thoroughly in the literature [1], [2], [14], even considering state constraints [16]. As mentioned previously, a concrete non-trivial example is considered in Section V.

In terms of the systems' interaction, it is assumed that each agent has access only to local information from a limited number of neighbors. This local interaction is represented by a graph, denoted $\mathcal{G} = (\mathcal{V}, \mathcal{E})$, where the set of nodes $\mathcal{V} := \{1, 2, \ldots, N\}$ corresponds to the labels of the agents and the set of edges $\mathcal{E} \subseteq \mathcal{V}^2$, of cardinality M, represents the communication between a pair of nodes —an edge e_k, $k \leq M$, is an ordered pair $(i, j) \in \mathcal{E}$ indicating that agent j has access to information from node i, via measurement or communication.

As mentioned in the Introduction, the exchange of information among the agents may be bidirectional or unidirectional. A bidirectional communication is represented by an *undirected* graph while an unidirectional exchange is modeled using a *directed* graph. In this paper we consider multi-agent systems communicating over undirected graphs, or two classes of directed graphs: spanning-trees or cycles. Furthermore, in realistic scenarios multi-agent systems are commonly subject to inter-agent constraints that may be defined as a set of restrictions on the system's output.

Without loss of generality, let the first component $x_{i,1}$ be the output for each agent, $i \leq N$ and define the relative-output state as

$$z_k := x_{i,1} - x_{j,1} \quad \forall k \leq M, \quad (i, j) \in \mathcal{E}. \tag{2}$$

For each $k \leq M$, let Δ_k and δ_k be, respectively, the upper and minimal distances, satisfying $0 \leq \delta_k < \Delta_k$. Then, the set of inter-agent output constraints is defined as

$$\mathcal{D} := \left\{ z \in \mathbb{R}^{nM} : \delta_k < |z_k| < \Delta_k, \ \forall\, k \leq M \right\}. \tag{3}$$

The control goal is for the agents to achieve output consensus with a non-zero displacement, centered at a point of non-predefined coordinates (as for instance in a formation control problem), in the presence of output constraints as given by the set $\mathcal{D}$ in (3). Mathematically, the consensus problem translates into making $x_{i,1} - x_{j,1} \to z_k^d$, or equivalently, $z_k \to z_k^d$ in the relative coordinates, where $z_k^d \in \mathbb{R}^n$ denotes the desired relative state between a pair of neighboring agents i and j. Note that setting $z_k^d \equiv 0$ corresponds to the output-consensus problem.

To address the consensus problem under constraints we use the edge-agreement framework for modeling of graphs [29]. In this framework the variables defined in (2) denote the states of the interconnection arcs in the graph, instead of those of the nodes, which are more commonly used. This has the advantage of recasting the consensus objective as the stabilization of the origin in error coordinates.

Let us denote the so-called incidence matrix of a graph by $E \in \mathbb{R}^{N \times M}$, which is a matrix with rows indexed by the nodes and columns indexed by the edges. Its (i, k)th entry is defined as follows: $[E]_{ik} := -1$ if i is the terminal node of edge e_k, $[E]_{ik} := 1$ if i is the initial node of edge e_k, and $[E]_{ik} := 0$ otherwise. Let $x_1^\top = \begin{bmatrix} x_{1,1}^\top \cdots x_{N,1}^\top \end{bmatrix} \in \mathbb{R}^{nN}$ be the collection of the first states, i.e., $l = 1$, of all the agents of the system. Then, the edge states in (2) satisfy

$$z := [E^\top \otimes I_n] x_1. \tag{4}$$

where $z^\top = [z_1^\top \cdots z_k \cdots z_M^\top]^\top \in \mathbb{R}^{nM}$, '$\otimes$' denotes the Kronecker product, and I_n the identity matrix of dimension $n \times n$. Similarly, an error variable is given by

$$\tilde{z} = [E^\top \otimes I_n] x_1 - z^d, \tag{5}$$

where $z^{d\top} = [z_1^{d\top} \cdots z_M^{d\top}] \in \mathbb{R}^{nM}$. Now, as before, let each $x_l^\top = \begin{bmatrix} x_{1,l}^\top \cdots x_{N,l}^\top \end{bmatrix} \in \mathbb{R}^{nN}$, $l \in \{2, \ldots, \rho\}$, be the collection of each state of all the agents of the system. Then, in the error edge coordinates, the consensus objective is that

$$\lim_{t \to \infty} \tilde{z}(t) = 0 \tag{6a}$$

$$\lim_{t \to \infty} x_l(t) = 0, \quad \forall l \in \{2, \ldots, \rho\}. \tag{6b}$$

Remark 1: Note that for $\rho = 2$ the objectives in (6) are equivalent to the output consensus of second-order multi-agent systems as it is commonly studied in the literature, e.g., on robot manipulators, mobile robots, etc. •

One of the advantages of considering the edge states rather than the node's is that it is possible to obtain an equivalent reduced system, easier to analyze using stability theory. Recall that, as observed in [29], using an appropriate labeling of the edges, the incidence matrix is expressed as

$$E = \begin{bmatrix} E_t & E_c \end{bmatrix} \tag{7}$$

where $E_t \in \mathbb{R}^{N \times (N-1)}$ denotes the full-column-rank incidence matrix corresponding to an arbitrary spanning tree $\mathcal{G}_t \subset \mathcal{G}$ and $E_c \in \mathbb{R}^{N \times (M-N+1)}$ represents the incidence matrix corresponding to the remaining edges not contained in $\mathcal{G}_t$. Moreover, defining

$$R := \begin{bmatrix} I_{N-1} & T \end{bmatrix} \tag{8}$$

with I_{N-1} denoting the $N-1$ identity matrix, and $T := \left(E_t^\top E_t\right)^{-1} E_t^\top E_c$, one obtains an alternative representation of the incidence matrix of the graph given by

$$E = E_t R. \tag{9}$$

The identity (9) is useful to derive a reduced-order dynamic model —cf. [29]. Now, as in the latter, the error edges' states may be split as

$$\tilde{z} = \begin{bmatrix} \tilde{z}_t^\top & \tilde{z}_c^\top \end{bmatrix}^\top, \quad \tilde{z}_t \in \mathbb{R}^{n(N-1)},\ \tilde{z}_c \in \mathbb{R}^{n(M-N+1)} \tag{10}$$

where $\tilde{z}_t$ are the states corresponding to the edges of an arbitrary spanning tree $\mathcal{G}_t$ and $\tilde{z}_c$ denote the states of the remaining edges, $\in \mathcal{G}\backslash\mathcal{G}_t$. Thus, after (4), (6), and (10), denoting $z_t^d \in \mathbb{R}^{n(N-1)}$ as the vector of desired relative displacements corresponding to $\mathcal{G}_t$, we obtain

$$\tilde{z} = \left[R^\top \otimes I_n\right]\tilde{z}_t. \tag{11}$$

Now, collecting the inputs of the multiple agents into the vector $u^\top = \begin{bmatrix} u_1^\top \cdots u_N^\top \end{bmatrix} \in \mathbb{R}^{nN}$ and the disturbances into $\theta_l^\top = \begin{bmatrix} \theta_{1,l}^\top \cdots \theta_{N,l}^\top \end{bmatrix} \in \mathbb{R}^{nN}$, with $l \in \{1, \ldots, \rho\}$, the reduced-order system's equations read

$$\dot{\tilde{z}}_t = \left[E_t^\top \otimes I_n\right]x_2 + \left[E_t^\top \otimes I_n\right]\theta_1(t) \tag{12a}$$
$$\dot{x}_l = x_{l+1} + \theta_l(t), \quad l \in \{2, \ldots, \rho-1\} \tag{12b}$$
$$\dot{x}_\rho = u + \theta_\rho(t). \tag{12c}$$

In these coordinates, output-consensus as defined in (6) is achieved if the origin is asymptotically stabilized for the reduced-order system (12). More precisely, consider the following problem.

Robust consensus problem with output constraints: Consider a multi-agent system of agents with high relative-degree dynamics given by (1), interacting over a connected undirected graph, a directed spanning tree or a directed cycle. Assume, in addition, that the systems are subject to inter-agent constraints that consist in the outputs being restricted to remain in the set defined in (3). Under these conditions, find a distributed dynamic controller with outputs u_i, $i \leq N$, that, in the absence of disturbances, i.e., $\theta_{i,l} \equiv 0$, $l \leq \rho$, $i \leq N$, achieves the objective (6) and renders the constraints set (3) forward invariant, i.e., $z(0) \in \mathcal{D}$ implies that $z(t) \in \mathcal{D}$ for all $t \geq 0$. Furthermore, in the presence of essentially bounded disturbances, that is $\theta_l \not\equiv 0$, u_i renders the origin of (12) practically input-to-state stable and the set $\mathcal{D}$ in (3) forward invariant. •

III. Control Design for Consensus under Output Constraints

The robust consensus problem with output constraints previously formulated is solved using a distributed dynamic nonlinear controller. Its design follows a backstepping approach that naturally exploits the normal form of the system. Hence, we start by defining a virtual control law for (12a), using x_2 as input. Now, in order to account for the output constraints, the design of the first virtual input for (12a), is based on the gradient of a *barrier Lyapunov function*. It is well known, however, that the backstepping approach may lead to an increase of complexity of the control law due to the successive differentiation of the virtual controllers [33]. This problem is emphasized by the fact that the said virtual control is designed as the gradient of a barrier function, which has multiple local minima and is defined only in open subsets of the state space. Therefore, in order to bypass these technical obstacles, inspired by the *command filtered backstepping* approach [34], we approximate the virtual inputs and their derivatives in each step of the backstepping design by means of command filters. This is explained in detail farther below.

A. Barrier Lyapunov function

Barrier Lyapunov functions are reminiscent of Lyapunov functions, so they are positive definite, but their domain of definition is restricted by design to open subsets of the Euclidean space. Furthermore, they grow unbounded as z_k approaches the boundary of their domain. We define them as follows —cf. [31].

Definition 1 (Barrier Lyapunov function): Consider the system $\dot{x} = f(x)$ and let $\mathcal{J}$ be an open set containing the origin. A Barrier Lyapunov function is a positive definite, function $V : \mathcal{J} \to \mathbb{R}_{\geq 0}$, $x \mapsto V(x)$, that is $\mathcal{C}^1$, satisfies

$$\nabla V(x)^\top f(x) := \frac{\partial V(x)}{\partial x}^\top f(x) \leq 0,$$

and has the property that $V(x) \to \infty$ and $|\nabla V(x)| \to \infty$ as $x \to \partial\mathcal{J}$. □

Now, akin to (3), for each $k \leq M$, the inter-agent constraints in terms of the error coordinates are given by the set

$$\tilde{\mathcal{D}}_k := \{\tilde{z}_k \in \mathbb{R}^n \,:\, \delta_k < |\tilde{z}_k + z_k^d| < \Delta_k\}.$$

Then, for each $k \leq M$, we define a barrier Lyapunov function candidate $W_k : \tilde{\mathcal{D}}_k \to \mathbb{R}_{\geq 0}$, of the form

$$W_k(\tilde{z}_k) = \frac{1}{2}\left[|\tilde{z}_k|^2 + B_k(\tilde{z}_k + z_k^d)\right], \tag{13}$$

where $B_k(\tilde{z}_k + z_k^d)$ is a non-negative function that satisfies: $B_k(z_k^d) = 0$, $\nabla B_k(z_k^d) = 0$, and $B_k(\tilde{z}_k + z_k^d) \to \infty$ as either $|\tilde{z}_k + z_k^d| \to \Delta_k$ or $|\tilde{z}_k + z_k^d| \to \delta_k$. Therefore, the barrier Lyapunov function candidate (13) satisfies: $W_k(\tilde{z}_k) \to \infty$ as either $|\tilde{z}_k + z_k^d| \to \Delta_k$ or $|\tilde{z}_k + z_k^d| \to \delta_k$, or equivalently in the original edge coordinates, as either $|z_k| \to \Delta_k$ or $|z_k| \to \delta_k$.

Remark 2: Note that the term $B_k(\tilde{z}_k + z_k^d)$ in (13) encodes the constraints on the original edge coordinates z_k in terms of the error $\tilde{z}_k$. This may lead to imposing conservative feasibility conditions in terms of the initial conditions when using, e.g., logarithmic barrier Lyapunov functions [47]. To overcome this limitation, $B(\tilde{z}_k + z_k^d)$ may be defined as an integral barrier Lyapunov function [47] or as a weight recentered barrier function [48], [49] —see also Section V. •

Remark 3: The functions defined in (13) are reminiscent of scalar potential functions in constrained environments [32] and, as for the latter, the appearance of multiple critical points is inevitable. Indeed, the gradient of the barrier Lyapunov function of the form (13), $\nabla W_k(\tilde{z}_k)$, vanishes at the origin and at an isolated saddle point separated from the origin — see Appendix I. Therefore, when using the gradient of (13) for

the control, the closed-loop system has multiple equilibrium points. This prevents us from using the classical stability tools for the analysis of the system. Such technical difficulty is addressed using tools tailored for so-called *multi-stable* systems—see [35], [36], and Appendix II. •

B. Control design for systems over directed graphs

Remark 4: For brevity, in the remainder of the paper we assume that the graph $\mathcal{G}$ representing the interaction topology is either a directed spanning tree or a directed cycle at the initial time. Nonetheless we stress that, with appropriate modifications, the results in this section also hold for undirected connected topologies. •

As mentioned earlier, the control design builds upon a recursive backstepping approach. Consider, first, the edge subsystem (12a) with x_2 as an input. In order to cope with the output constraints, a good choice of control law consists, as mentioned previously, in the gradient of a barrier function [21], [50], [51]. As it is defined here in edge coordinates, specific notations are introduced.

Let us define the so-called in-incidence matrix $E_\odot \in \mathbb{R}^{N\times M}$, whose elements are defined as follows—cf. [52]—: $[E_\odot]_{ik} := -1$ if i is the terminal node of edge e_k and $[E_\odot]_{ik} := 0$ otherwise. Similarly the elements of so-called out-incidence matrix $E_\otimes \in \mathbb{R}^{N\times M}$ are defined as follows: $[E_\odot]_{ik} := 1$ if i is the initial node of edge e_k and $[E_\odot]_{ik} := 0$ otherwise. Then, in the edge agreement framework the consensus control based on the gradient of the barrier function is given by[1]

$$x_2^* := -c_1[E_\odot \otimes I_n]\nabla W(\tilde{z}), \tag{14}$$

where c_1 is a constant that is positive by design and $\nabla W(\tilde{z})$ is the gradient of a barrier Lyapunov function for the multi-agent system, which is defined as

$$W(\tilde{z}) = \sum_{k\leq M} W_k(\tilde{z}_k), \tag{15}$$

with $W_k(\tilde{z}_k)$ given in (13) for all $k \leq M$. Indeed, the right-hand side of (14) qualifies as a consensus control law that guarantees connectivity maintenance for first-order multi-agent systems $\dot{\tilde{z}}_t = u$ interconnected over directed graphs —cf. [53]. So, defining $\bar{x}_2 := x_2 - x_2^*$ and using (14), Equation (12a) becomes[2]

$$\dot{\tilde{z}}_t = -c_1[E_t^\top E_\odot \otimes I_n]\nabla W(\tilde{z}) + [E_t^\top \otimes I_n]\left[\bar{x}_2 + \theta_1\right]. \tag{16}$$

With aim at making $\bar{x}_2 \to 0$ in (16), following a backstepping-based design, we rewrite the second equation in (12b), i.e., with $l = 2$, in error coordinates $\bar{x}_2$ and we consider x_3 as an input. We have

$$\dot{\bar{x}}_2 = x_3 - \dot{x}_2^* + \theta_2. \tag{17}$$

Hence, the natural virtual control law at this stage is

$$x_3^* = -c_2\bar{x}_2 + \dot{x}_2^*, \quad c_2 > 0, \tag{18}$$

[1]For undirected graphs this virtual control law takes the form $x_2^* = -c_1[E \otimes I_n]\nabla W(\tilde{z})$, where E is the incidence matrix—cf. [21].

[2]To avoid a cumbersome notation we write $\nabla W(\tilde{z})$ in place of the more appropriate spelling $\nabla W(\left[R^\top \otimes I_n\right]\tilde{z}_t)$.

which requires the derivative of the right-hand side of (14). Furthermore, a recursive procedure requires up to $\rho - 2$ successive derivatives of x_2^*, which posses significant technical and numerical difficulties. Thus, to avoid the use of successive derivatives of $\nabla W(\tilde{z})$ we approximate the derivatives of the virtual controls x_l^*, with $l \in \{2, \ldots, \rho - 1\}$ by means of *command filters*. For simplicity, we use second-order systems defined as in the figure below —cf. [34];

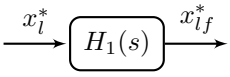

$$H_1(s) := \frac{\omega_n^2}{s^2 + 2\omega_n s + \omega_n^2}$$

Fig. 1: Command filter used for implementation. The dirty derivative of x_l^* may be obtained using $\dot{x}_{lf} := sH_1(s)x_l^*$ which is equivalent to $\dot{x}_{lf} = H_1(s)\dot{x}_l^*$.

The virtual controls are considered as the inputs of a command filter, with the outputs corresponding to the approximated signals and their derivatives, denoted x_{lf} and $\dot{x}_{lf}$, respectively. The filters' natural frequency, $\omega_n > 0$, is a control parameter which is chosen large enough so that the approximation x_{lf} converges to the desired virtual control x_l^* in a faster time-scale than that of the system's dynamics — see Section IV-A. Moreover, the filters are designed with unit DC gain and unit damping coefficient so that the tracking of the virtual signals is guaranteed without overshoot. This ensures that, in the slower time-scale of the systems' dynamics, the "filtered forms" act as the desired virtual signals, corresponding to a classical backstepping control. Similarly, $\dot{x}_{lf} = H_1(s)\dot{x}_l^*$ approximates $\dot{x}_l^*$.

Remark 5: For clarity, we use second-order command-filters as defined in Fig. 1 above. However, the design is not restricted to this particular choice. Indeed, other possibilities include first-order low-pass filters [54] or high-order Levant differentiators [26]. •

For the purpose of stability analysis, we write the command filters' dynamics in state form. To that end, let the filters' variables be denoted as $\alpha_{l-1}^\top := \left[\alpha_{l-1,1}^\top\ \alpha_{l-1,2}^\top\right] \in \mathbb{R}^{2nN}$, for $l \in \{2, \ldots, \rho\}$. Then, in state-space representation, the command filters are written as

$$\dot{\alpha}_{l-1} = \omega_n\left[A \otimes I_{nN}\right]\alpha_{l-1} + \omega_n\left[B \otimes I_{nN}\right]x_l^* \tag{19a}$$

$$\left[x_{lf}^\top\ \dot{x}_{lf}^\top\right]^\top = \left[C \otimes I_{nN}\right]\alpha_{l-1}, \quad l \in \{2, \ldots, \rho\}, \tag{19b}$$

$$A := \begin{bmatrix} 0 & 1 \\ -1 & -2 \end{bmatrix}, \quad B := \begin{bmatrix} 0 \\ 1 \end{bmatrix}, \quad C := \begin{bmatrix} 1 & 0 \\ 0 & \omega_n \end{bmatrix} \tag{19c}$$

and the initial conditions are set to $\alpha_{l-1,1}(0) = x_l^*(0)$ and $\alpha_{l-1,2}(0) = 0$.

Thus, the virtual control input, starting with (18), are redefined using the filter variables as follows. First, we redefine

$$x_3^* := -c_2\tilde{x}_2 + \dot{x}_{2f} \tag{20}$$

where $\tilde{x}_2 := x_2 - x_{2f}$ and $\dot{x}_{2f} = \omega_n\alpha_{1,2}$. Hence, in contrast to (17), from

$$\dot{x}_2 - \dot{x}_{2f} = x_3 - \dot{x}_{2f} + \theta_2 + x_3^* - x_3^* + \alpha_{2,1} - \alpha_{2,1},$$

defining $\tilde{x}_3 := x_3 - x_{3f}$ and using (20) and $\alpha_{2,1} = x_{3f}$, we obtain

$$\dot{\tilde{x}}_2 = -c_2\tilde{x}_2 + \tilde{x}_3 + (\alpha_{2,1} - x_3^*) + \theta_2.$$

Then, owing to the fact that the system is in feedback form, we define

$$x_l^* := -c_{l-1}\tilde{x}_{l-1} + \omega_n\alpha_{l-2,2} - \tilde{x}_{l-2}, \quad l \in \{4, \dots, \rho\}, \tag{21}$$

where c_2, c_{l-1} are positive constants, and the tracking errors are given by

$$\tilde{x}_l := x_l - x_{lf} = x_l - \alpha_{l-1,1}, \quad l \in \{2, \dots, \rho\} \tag{22}$$

—cf. Eq. (20). That is, the virtual controls x_l^* starting from $l = 3$ are redesigned to steer x_{l-1} towards the *filtered* virtual input $x_{l-1\,f}$. Finally, the actual control input is set to

$$u = -c_\rho\tilde{x}_\rho + \omega_n\alpha_{\rho-2,2} - \tilde{x}_{\rho-1}. \tag{23}$$

Remark 6: The system being in feedback form, the third term on the right-hand side of (21) and (23) are *feedback passivation* terms —cf. [55]. These terms, that come from the *backstepping-as-recursive-feedback-passivation* approach [56] are used to render the system (12) passive with respect to the output $y_\rho := x_\rho - x_{\rho f}$. •

Thus, taking the derivative of the backstepping error variables defined in (22) and using the input (23), with (19)-(21), we obtain the closed-loop system

$$\begin{aligned}
\dot{\tilde{z}}_t =& -c_1[E_t^\top E_\odot \otimes I_n]\nabla W(\tilde{z}) \\
&+ [E_t^\top \otimes I_n]\left[\tilde{x}_2 + (\alpha_{1,1} - x_2^*) + \theta_1\right] && \text{(24a)}\\
\dot{\tilde{x}}_2 =& -c_2\tilde{x}_2 + \tilde{x}_3 + (\alpha_{2,1} - x_3^*) + \theta_2 && \text{(24b)}\\
\dot{\tilde{x}}_l =& -c_l\tilde{x}_l + \tilde{x}_{l+1} - \tilde{x}_{l-1} + (\alpha_{l,1} - x_{l+1}^*) + \theta_l, \\
&\qquad \forall\, l \in \{3, \dots, \rho-1\} && \text{(24c)}\\
\dot{\tilde{x}}_\rho =& -c_\rho\tilde{x}_\rho - \tilde{x}_{\rho-1} + \theta_\rho && \text{(24d)}\\
\dot{\alpha}_l =& \omega_n\left[A \otimes I_{nN}\right]\alpha_l + \omega_n\left[B \otimes I_{nN}\right]x_{l+1}^*, \\
&\qquad \forall\, l \in \{1, \dots, \rho-1\}. && \text{(24e)}
\end{aligned}$$

Consequently, solving the robust consensus problem with output constraints comes to guaranteeing that $\tilde{z}_t(t)$, as part of the solution to Eqs. (24), tends to zero. More precisely, that the control law (23), with (14) and (19)-(21), solves the robust consensus problem with output constraints for system (1) is a fact established by the following statement.

Theorem 1: Consider the system (1) in closed loop with the dynamic controller defined by (23), together with (14) and (19)-(21). Then, the constraints set (3) is forward invariant. Moreover, if $\theta_{i,l} \equiv 0$, $l \leq \rho$, $i \leq N$, (6) holds for almost all initial conditions satisfying $z(0) \in \mathcal{D}$. Otherwise, if $\theta_l \not\equiv 0$, the closed-loop system is almost-everywhere practically input-to-state stable with respect to $\theta := [\theta_1^\top \cdots \theta_\rho^\top]^\top$. □

For clarity of exposition, the proof of Theorem 1 is presented in Section IV, but in anticipation of the latter we underline the following. As mentioned earlier, part of the control approach consists in choosing ω_n sufficiently large, so that $\alpha_{l-1,1} \to x_l^*$ faster than the dynamics of the system. Note that, setting $\epsilon := 1/\omega_n$ as a *singular* parameter in (39a), the closed-loop system (24) may be separated into two time scales, where the fast system corresponds to the command filters. Hence, when $\alpha_{l-1,1} = x_l^*$ and $\alpha_{l-1,2} = 0$, the reduced slow system, corresponding to the actual system with the backstepping control, effectively achieves consensus with respect of the output constraints.

The proposed controller and stability analysis offer some advantages with respect to previous results in the literature. Using the reduction of the edge system considering only the states of a spanning tree contained in the graph, we are able to analyze the system using Lyapunov and input-to-state stability theory (in a multi-stability sense [35], [36]) of the reduced slow system. The latter is significant since the reduced slow system corresponds to a high-order system in closed-loop with a classical backstepping controller solving the output-constrained consensus problem. On the other hand, relying on the multi-stability framework for singularly perturbed systems, it is possible to establish not only convergence to the consensus manifold but also explicit robustness properties in the sense of practical input-to-state stability with respect to bounded disturbances.

C. Extension to partial- and full-state consensus with output constraints

The control design methodology presented above can be directly extended to consider consensus in all or part of the high-order states x_l. This is useful, for instance, in the context of flocking in formation, attitude consensus, etc.

Suppose that, besides achieving the output-consensus goal as defined in (6a), it is additionally required to achieve consensus of a number of states $r \leq \rho$. For convenience, and without loss of generality, suppose that $3 < r < \rho$. Then, akin to the edge transformation (4), we define the edge states

$$z_l := [E^\top \otimes I_n]x_l, \quad l \in \{2, \dots, r\} \tag{25}$$

and, accordingly, let the objectives in (6) be replaced with

$$\begin{aligned}
&\lim_{t\to\infty} \tilde{z}(t) = 0 && \text{(26a)}\\
&\lim_{t\to\infty} z_l(t) = 0, \quad \forall l \in \{2, \dots, r\} && \text{(26b)}\\
&\lim_{t\to\infty} x_l(t) = 0, \quad \forall l \in \{r+1, \dots, \rho\}. && \text{(26c)}
\end{aligned}$$

Furthermore, let

$$\begin{aligned}
\tilde{z}_l :=& z_l - [E^\top \otimes I_n]x_{lf} \quad \forall\, l \in \{2, \dots, r\} && \text{(27)}\\
\tilde{x}_l :=& x_l - x_{lf} \quad \forall\, l \in \{r+1, \dots, \rho\}; && \text{(28)}
\end{aligned}$$

we recall that $x_{lf} = \alpha_{l-1,1}$. Then, to achieve the new consensus objectives (26) the virtual control inputs, at each step, are redefined as

$$z_l^* := [E^\top \otimes I_n]x_l^*, \quad \forall\, l \in \{2, \dots, r\} \tag{29}$$

with x_2^* as in (14), $x_3^* := -c_2[E_\odot \otimes I_n]\tilde{z}_2 + \omega_n\alpha_{1,2}$,

$$x_l^* := -c_{l-1}[E_\odot \otimes I_n]\tilde{z}_{l-1} + \omega_n\alpha_{l-2,2} - \tilde{x}_{l-2}$$

for all $l \in \{4, \dots, r\}$, and

$$\begin{aligned}
x_{r+1}^* :=& -c_r[E_\odot \otimes I_n]\tilde{z}_r + \omega_n\alpha_{r-1,2} - [E_\odot \otimes I_n]\tilde{z}_{r-1}, && \text{(30)}\\
x_l^* :=& -c_{l-1}\tilde{x}_{l-1} + \omega_n\alpha_{l-2,2} - \tilde{x}_{l-2}, \quad l \in \{r+2, \dots, \rho\}. && \text{(31)}
\end{aligned}$$

Finally, the actual control input is set to

$$u := -c_\rho \tilde{x}_\rho + \omega_n \alpha_{\rho-2,2} - \tilde{x}_{\rho-1}. \tag{32}$$

Then, we have the following.

Theorem 2: Consider the system (1) in closed loop with the dynamic controller defined by (32), together with (29)-(31) and (19). Then, the constraints set (3) is forward invariant. Moreover, if $\theta_{i,l} \equiv 0$, $l \leq \rho$, $i \leq N$, the limits in (26) hold for almost all initial conditions satisfying $z(0) \in \mathcal{D}$. Otherwise, if $\theta_l \not\equiv 0$, the closed-loop system is almost-everywhere practically input-to-state stable with respect to $\theta := [\theta_1^\top \cdots \theta_\rho^\top]^\top$. □

Modulo the change to the reduced-edge coordinates—see (11)—for the higher-order edge states, the proof is identical to the proof of Theorem 1, which is presented next.

IV. Proof of Theorem 1

The proof is organized in two main parts. In the first part, we show how the closed-loop system (24) can be written as a singularly-perturbed system with singular parameter $\epsilon := 1/\omega_n$ and in which the fast systems correspond to the dynamics of the command filters and the slow system corresponds to the high-order dynamics of the original multi-agent system. In the second part we analyze the stability and the robustness of the singularly perturbed system, using analysis tools multi-stable systems theory [35], [36].

A. Singular perturbation model

Define $\alpha^\top := \begin{bmatrix}\alpha_1^\top & \cdots & \alpha_{\rho-1}^\top\end{bmatrix} \in \mathbb{R}^{2nN(\rho-1)}$, $\xi^\top := \begin{bmatrix}\tilde{z}_t^\top & \tilde{x}_2^\top & \cdots & \tilde{x}_\rho\end{bmatrix}^\top \in \mathbb{R}^{n(\rho N-1)}$, and $\theta^\top := [\theta_1 \cdots \theta_\rho] \in \mathbb{R}^{n\rho N}$. Then, the filter subsystem (24e) can be rewritten as

$$\dot{\alpha} = \omega_n \tilde{A}\big[\alpha - \chi(\xi,\alpha)\big], \quad \tilde{A} := \text{blockdiag}\{[A \otimes I_{nN}]\}, \tag{33}$$
$$\chi(\xi,\alpha) := \begin{bmatrix}x_2^{*\top} & 0^\top & x_3^{*\top} & 0^\top & \cdots & x_\rho^{*\top} & 0^\top\end{bmatrix}^\top.$$

Now, as mentioned in the previous section, with $\epsilon := 1/\omega_n$ as the singular parameter, the closed-loop system (24) may be written in the singular-perturbation form

$$\dot{\xi} = f(\xi,\alpha,\theta,\epsilon) \tag{34a}$$
$$\epsilon\dot{\alpha} = g(\xi,\alpha,\theta,\epsilon). \tag{34b}$$

Setting $\epsilon = 0$ in (34) we obtain the so-called quasi-state model

$$\dot{\xi} = f(\xi,\alpha,\theta,0) \tag{35a}$$
$$0 = g(\xi,\alpha,\theta,0) \tag{35b}$$

in which (35b) becomes an algebraic equation. Hence, the analysis of the singular perturbation model (34) is normally conducted studying its dynamic properties in different time scales [46].

Denote $\alpha_s = h(\xi)$ the unique root of the algebraic equation (35b),

$$h(\xi) = \Big[(-c_1[E_\odot \otimes I_n]\nabla W(\tilde{z}))^\top \;\; 0^\top \;\; -c_2\tilde{x}_2^\top \;\; 0^\top \;\; \cdots \;\; -c_{\rho-1}\tilde{x}_{\rho-1}^\top \;\; 0^\top\Big]^\top. \tag{36}$$

Then, defining the coordinate transformation

$$\tilde{\alpha} := \begin{bmatrix}\tilde{\alpha}_{1,1}^\top & \tilde{\alpha}_{1,2}^\top & \cdots & \tilde{\alpha}_{\rho-1,1}^\top & \tilde{\alpha}_{\rho-1,2}^\top\end{bmatrix}^\top = \alpha - h(\xi), \tag{37}$$

and using (24) we obtain the singularly perturbed system

$$\dot{\tilde{z}}_t = -c_1[E_t^\top E_\odot \otimes I_n]\nabla W(\tilde{z}) + [E_t^\top \otimes I_n]\,[\tilde{x}_2 + \tilde{\alpha}_{1,1} + \theta_1] \tag{38a}$$
$$\dot{\tilde{x}}_2 = -c_2\tilde{x}_2 + \tilde{x}_3 + \tilde{\alpha}_{2,1} + \theta_2 \tag{38b}$$
$$\dot{\tilde{x}}_l = -c_l\tilde{x}_l + \tilde{x}_{l+1} - \tilde{x}_{l-1} + \tilde{\alpha}_{l,1} + \theta_l, \quad l = 3,\ldots,\rho-1 \tag{38c}$$
$$\dot{\tilde{x}}_\rho = -c_\rho\tilde{x}_\rho - \tilde{x}_{\rho-1} + \theta_\rho \tag{38d}$$
$$\epsilon\dot{\tilde{\alpha}} = \tilde{A}\tilde{\alpha} - \epsilon\frac{\partial h(\xi)}{\partial \xi}\dot{\xi}. \tag{38e}$$

In turn, the reduced system $\dot{\xi} = f(\xi, h(\xi), \theta, 0)$ takes the form

$$\dot{\tilde{z}}_t = -c_1[E_t^\top E_\odot \otimes I_n]\nabla W(\tilde{z}) + [E_t^\top \otimes I_n]\,[\tilde{x}_2 + \theta_1] \tag{39a}$$
$$\dot{\bar{x}} = -[H \otimes I_{nN}]\bar{x} + \bar{\theta}, \tag{39b}$$

where $\bar{x}^\top := \begin{bmatrix}\tilde{x}_2^\top & \cdots & \tilde{x}_\rho^\top\end{bmatrix}$, $\bar{\theta}^\top := \begin{bmatrix}\theta_2^\top & \cdots & \theta_\rho^\top\end{bmatrix}$, and

$$H := \begin{bmatrix} c_2 & -1 & 0 & \cdots & 0 \\ 1 & c_3 & -1 & \cdots & 0 \\ \vdots & \ddots & \ddots & \ddots & \vdots \\ 0 & \ldots & 1 & c_{\rho-1} & -1 \\ 0 & \ldots & 0 & 1 & c_\rho \end{bmatrix}. \tag{40}$$

On the other hand, the boundary layer system, $(d\tilde{\alpha}/d\tau) = g(\xi, \tilde{\alpha} + h(\xi), \theta, 0)$, with $\tau = t/\epsilon$ and with ξ considered as fixed, is

$$\frac{d\tilde{\alpha}}{d\tau} = \tilde{A}\tilde{\alpha} \tag{41}$$

where $\tilde{A}$ is a Hurwitz matrix —see Eqs. (33) and (19c).

Even though the system (38) appears to be in the familiar form (34), its analysis is stymied by the fact that the function ∇W vanishes at multiple separate equilibria. Therefore, we rely on perturbation theory for multi-stable systems, developed in [35]. The stability analysis is provided below and some definitions and statements from [35] are recalled in Appendix II, for convenience.

B. Stability and robustness analysis

Denote $\tilde{z}_t^* \in \mathbb{R}^{n(N-1)}$ as the vector containing the saddle points of the barrier Lyapunov function for each edge (13). Then, the equilibrium points of subsystem (38a) are collected into a disjoint set, denoted by

$$\mathcal{W} := \{0\} \cup \{\tilde{z}_t^*\}, \tag{42}$$

which is an acyclic $\mathcal{W}$-limit set[3] of (38a). This means that asymptotic stability of the origin of (38a) may be guaranteed, at best, almost everywhere in $\mathcal{D}$, that is, for all initial conditions in $\mathcal{D}$ except for a set of measure zero corresponding to the domain of attraction of the unstable critical point.

[3]In the settings of this paper an acyclic limit set corresponds to an invariant set of isolated points in Euclidean space. See [35] for a complete definition.

Now, we first analyze the stability of (38) with respect to the set of equilibria $\mathcal{W}_\Theta := \mathcal{W} \times \{0\}^{\rho-1}$. For this purpose we use Theorem 3 in Appendix II, which is essentially a reformulation of [35, Theorem 2] adapted to the contents of this paper. Theorem 3 establishes sufficient conditions for a practical input-to-state multi-stability property to hold for a singularly perturbed system with respect to $\mathcal{W}_\Theta$ and to a bounded external input θ, granted that the reduced system (39) is input-to-state stable with respect to set $\mathcal{W}_\Theta$ and input θ and that the origin for (41) is globally asymptotically stable. Therefore, the stability and robustness analysis is conducted in the following steps:

1) We show that the origin is asymptotically stable for the boundary layer system (41).
2) Relying on the results on cascaded multi-stable systems in [36], we show that the reduced system (39) is input-to-state stable with respect to set $\mathcal{W}_\Theta$ and input θ.
3) Using Theorem 3 in Appendix II, we prove that, for a sufficiently small ϵ, the singularly perturbed system (38) is practically input-to-state stable with respect to the set $\mathcal{W}_\Theta \times \{0\}$ and a bounded external input θ. Moreover, using [35, Theorem 3], in the absence of disturbances, we show convergence to the set of equilibria.
4) Using the practical input-to-state multi-stability property, we establish almost-everywhere-practical-input-to-state stability of the origin of (38). Similarly, if $\theta \equiv 0$, we establish convergence to the origin.
5) Finally, we show that the output-constraints set defined in (3) is forward invariant.

Step 1) Since $\tilde{A}$ is Hurwitz by design, the origin $\tilde{\alpha} = 0$ is exponentially stable for the boundary-layer system (41).

Step 2) Consider the reduced system (39). Note that it has the form of a cascaded system, in which (39b) is the "driving" system and the "driven" system (39a) has multiple equilibria given by the set $\mathcal{W}$ in (42). In order to prove input-to-state stability of (39) with respect to set $\mathcal{W}_\Theta$ and input θ, as per in [36], we need to show that (39a) is input-to-state stable with respect to the set $\mathcal{W}$ and the inputs $\tilde{x}_2$ and θ_1 whereas the system (39b) is input-to-state stable with respect to $\bar{\theta}$. We start with the latter.

Input-to-state stability with respect to $\bar{\theta}$ for the system (39b) follows directly from Lyapunov theory since (39b) is a linear time-invariant system and $-[H \otimes I_{nN}]$ is Hurwitz matrix, since so is $-H$.

Consider, in turn, the reduced subsystem (39a). For this system we use the barrier Lyapunov function $W(\tilde{z})$ given by (15). First note that $W(\tilde{z})$ consists in a sum of the barrier Lyapunov functions defined for each edge in the initial graph. Yet, from the identity (11) it is possible to express W in terms of the edges corresponding to a spanning tree contained in the graph. Hence, define the candidate Lyapunov function

$$V_z(\tilde{z}_t) = W\big(\left[R^\top \otimes I_n\right] \tilde{z}_t\big).$$

On the other hand, for consistency in the notation, we define the constraint set (3) in terms of the edges of the spanning tree z_t as

$$\mathcal{D}_t := \big\{z_t \in \mathbb{R}^{n(N-1)} : \big|\left[r_k^\top \otimes I_n\right] z_k\big| \in (\delta_k, \Delta_k),\ \forall\, k \leq M\big\}$$

where r_k is the kth column of R in (8). For the time-being, assume that $\mathcal{D}$ (equivalently $\mathcal{D}_t$) is forward invariant; this hypothesis is relaxed below. Then, for all $\tilde{z}_t \in \mathcal{D}_t$, $V_z(\tilde{z}_t)$ satisfies

$$\frac{1}{2}|\tilde{z}_t|_{\mathcal{W}}^2 \leq V_z(\tilde{z}_t), \tag{43}$$

where $|\tilde{z}_t|_{\mathcal{W}} = \min\{|\tilde{z}_t|, |\tilde{z}_t - \tilde{z}_t^*|\}$. Furthermore, from (39a), the derivative of V_z is given by

$$\begin{aligned}\dot{V}_z =& -c_1 \nabla W(\tilde{z}) \left[R^\top E_t^\top E_\odot \otimes I_n\right] \nabla W(\tilde{z}) \\ &+ \nabla W(\tilde{z})^\top \left[R^\top E_t^\top \otimes I_n\right] [\tilde{x}_2 + \theta_1],\end{aligned} \tag{44}$$

where R is defined in (8). Equation (44) holds for, both, directed-spanning-tree and directed-cycle topologies. Next, we analyze the two considered topologies separately.

Case 1 (Directed spanning tree). In this case we have $\mathcal{G} = \mathcal{G}_t$. Therefore, $z = z_t$, $E = E_t$, and $R = I_{N-1}$. Hence, (44) becomes

$$\begin{aligned}\dot{V}_z =& -c_1 \nabla W(\tilde{z}_t) \left[E_t^\top E_\odot \otimes I_n\right] \nabla W(\tilde{z}_t) \\ &+ \nabla W(\tilde{z}_t)^\top \left[E_t^\top \otimes I_n\right] [\tilde{x}_2 + \theta_1]\end{aligned} \tag{45}$$

Define $L_e^s := \frac{1}{2}\left(E_t^\top E_\odot + E_\odot^\top E_t\right)$, which is the symmetric part of the so-called directed edge Laplacian $E_t^\top E_\odot$. As it is shown in the proof of Proposition 1 in [53], L_e^s is positive definite. Therefore, applying Young's inequality to the second term in the right-hand side of (45), we have

$$\dot{V}_z \leq -\, c_1' |\nabla V_z(\tilde{z}_t)|^2 + \frac{1}{2\gamma}\left[|\tilde{x}_2|^2 + |\theta_1|^2\right], \tag{46}$$

where $c_1' := \left[c_1\, \lambda_{min}(L_e^s) - \frac{\gamma \lambda_{max}(E_t^\top E_t)}{2}\right]$ is positive for a sufficiently small $\gamma > 0$, $\lambda_{min}(L_e^s) > 0$ is the smallest eigenvalue of L_e^s, and $\lambda_{max}(E_t^\top E_t)$ is the largest eigenvalue of $E_t^\top E_t$.

Case 2 (Directed cycle). Consider equation (44). Using the identity (9), we have

$$\begin{aligned}\dot{V}_z =& -c_1 \nabla W(\tilde{z}) \left[E^\top E_\odot \otimes I_n\right] \nabla W(\tilde{z}) \\ &+ \nabla W(\tilde{z})^\top \left[E^\top \otimes I_n\right] [\tilde{x}_2 + \theta_1].\end{aligned} \tag{47}$$

Now, for a directed-cycle topology, the following identity follows —cf. [53]—

$$E^\top E_\odot + E_\odot^\top E = E^\top E. \tag{48}$$

Therefore, using (48) and (9) again, we have

$$\begin{aligned}\dot{V}_z =& -\frac{c_1}{2} \nabla W(\tilde{z}) \left[\left(E^\top E_\odot + E_\odot^\top E\right) \otimes I_n\right] \nabla W(\tilde{z}) \\ &+ \nabla W(\tilde{z})^\top \left[R^\top E_t^\top \otimes I_n\right] [\tilde{x}_2 + \theta_1] \\ =& -\frac{c_1}{2} \nabla W(\tilde{z}) \left[R^\top E_t^\top E_t R^\top \otimes I_n\right] \nabla W(\tilde{z}) \\ &+ \nabla W(\tilde{z})^\top \left[R^\top E_t^\top \otimes I_n\right] [\tilde{x}_2 + \theta_1].\end{aligned} \tag{49}$$

Denote

$$\nabla V_z(\tilde{z}_t) := \frac{\partial V_z(\tilde{z}_t)}{\partial \tilde{z}_t} = [R \otimes I_n] \nabla W(\left[R^\top \otimes I_n\right] \tilde{z}_t). \tag{50}$$

Then, applying Young's inequality to the second term of the right-hand side of (49), we have

$$\dot{V}_z \leq -\, c_1' |\nabla V_z(\tilde{z}_t)|^2 + \frac{1}{2\gamma}\left[|\tilde{x}_2|^2 + |\theta_1|^2\right], \tag{51}$$

where $c_1' := \frac{\lambda_{min}(E_t^\top E_t)}{2}[c_1 - \gamma]$ is positive for a sufficiently small $\gamma > 0$. Note that, $\lambda_{min}(E_t^\top E_t)$ is positive since it is the smallest eigenvalue of the edge Laplacian of an undirected spanning tree —cf. [21].

Thus, for either the spanning tree or the cycle case, the derivative of $V_z(z_t)$ satisfies

$$\dot{V}_z \leq -c_1'|\tilde{z}_t|^2_{\mathcal{W}} + \frac{1}{2\gamma}\left[|\tilde{x}_2|^2 + |\theta_1|^2\right]. \tag{52}$$

It follows from (43), (52), and Theorem 4 in Appendix II, that the subsystem (39a) is input-to-state stable with respect to the set of equilibria $\mathcal{W}$, and the inputs $\tilde{x}_2$ and θ_1.

Thus, after [36, Theorem 3.1], the reduced system (39) is input-to-state stable with respect to $\mathcal{W}_\Theta$ and input θ. Furthermore, $\mathcal{W}_\Theta$ qualifies as a $\mathcal{W}$-limit set for (39).

Step 3) Since the reduced system (39) is input-to-state stable with respect to $\mathcal{W}_\Theta$ and θ, and the origin of (41) is asymptotically stable, it follows, after Theorem 3 in Appendix II, that the singularly perturbed system (38) is practically input-to-state stable with respect to set $\mathcal{W}_\Theta \times \{0\}^{2nN(\rho-1)}$ and input θ. More precisely, for any pair of constants d_1, $d_2 > 0$, there exists an $\epsilon^* > 0$ such that, for any $\epsilon \in (0, \epsilon^*]$, the solutions of (38) satisfy

$$\limsup_{t\to\infty} |\xi(t)|_{\mathcal{W}_\Theta} \leq \eta_\theta(\|\theta\|_\infty) + d_2 \tag{53a}$$

$$|\tilde{\alpha}(t)| \leq \beta_\alpha\left(|\tilde{\alpha}(0)|, \frac{t}{\epsilon}\right) + d_2, \quad \forall\, t \geq 0, \tag{53b}$$

provided that

$$\max\{|\xi(0)|_{\mathcal{W}_\Theta}, |\tilde{\alpha}(0)|, \|\theta\|_\infty, \|\dot{\theta}\|_\infty\} \leq d_1,$$

where $\|\theta\|_\infty := \limsup_{t\to\infty} \|\theta(t)\|$ and $|\xi|_{\mathcal{W}_\Theta} := \inf_{a\in\mathcal{W}_\Theta} |\xi - a|$.

Now consider the case in which the disturbance $\theta \equiv 0$. From property (53a) we may conclude that the origin of the reduced system (39) is multi-stable with respect to $\mathcal{W}_\Theta$. Therefore, from the latter and the exponential stability of the boundary layer system (41) all the assumptions of [35, Theorem 3] are satisfied and the solutions of (38) satisfy

$$\lim_{t\to\infty} |\xi(t)|_{\mathcal{W}_\Theta} = 0 \tag{54a}$$

$$\lim_{t\to\infty} |\tilde{\alpha}(t)| = 0. \tag{54b}$$

Step 4) Since the critical point $\tilde{z}_t^*$ of the barrier function is a saddle point —see Appendix I, after [57, Proposition 11], it follows that the region of attraction of the unstable equilibrium $\tilde{z}_t^*$ has zero Lebesgue measure. Therefore, we conclude that the bound in (53a) and the limit in (54a) are satisfied for the origin $\{\xi = 0\}$. More precisely, we have

$$\limsup_{t\to\infty} |\xi(t)| \leq \eta_\theta(\|\theta\|_\infty) + d_2$$

and, for $\theta \equiv 0$,

$$\lim_{t\to\infty} |\xi(t)| = 0.$$

Step 5) Up to this point we have assumed that the inter-agent constraints are satisfied for all time, that is, $z(t) \in \mathcal{D}$ for all $t \geq 0$. Then, in order to prove the forward invariance of the constraints set we proceed by contradiction as follows. Assume that the state constraints are not respected. Therefore, from continuity of the solutions, there exists a time $T > 0$ such that $z_t(T) \in \partial\mathcal{D}_t$. Now, from the previous analysis of the singularly perturbed system, we have that in the interval $[0, T)$, condition (91b) holds. Moreover, since $\tilde{\alpha}(0) = 0$ by design, the solutions of the filter error satisfy $\tilde{\alpha}(t) \leq d_2$, for $t \in [0, T)$. Consider the derivative of the Lyapunov function (43) along the trajectories of (38a), which satisfies

$$\dot{V}_z(\tilde{z}_t) \leq -c_1'|\nabla V_z(\tilde{z}_t)|^2 + \frac{1}{2\gamma}\left[|\tilde{x}_2|^2 + |\theta_1|^2 + |\tilde{\alpha}|^2\right]$$

Therefore, since $\tilde{\alpha}(t) \leq d_2$, $\theta_1(t)$ is bounded and the system in (39b) is input-to-state stable, $\tilde{x}_2(t)$ is bounded, for all $t \in [0, T)$. Then, we have

$$\dot{V}_z(\tilde{z}_t(t)) \leq -c_1'|\nabla V_z(\tilde{z}_t(t))|^2 + d, \quad \forall t \in [0, T)$$

where d is a positive constant. By Definition 1 we have $|\nabla V(\tilde{z}_t(t))| \to \infty$ as $z_t(t)$ approaches the border of the constraints set, $\partial\mathcal{D}_t$. Therefore, if $|\tilde{z}_t(t)|$ grows, there exists a time $0 < T^* < T$ such that $\dot{V}_z(\tilde{z}_t(T^*)) \leq 0$. The latter, in turn means that $V_z(\tilde{z}_t(t))$ is bounded for all $t \in [0, T)$, which contradicts the initial assumption that the constraints are not respected. By resetting the initial conditions, the previous reasoning can be repeated for $t \geq T$. Therefore, the interval where $V_z(\tilde{z}_t(t))$ is bounded can be extended to infinity. The boundedness of $V_z(\tilde{z}_t(t))$ means, based on the definition of the barrier Lyapunov function, that the constraints are always respected or, equivalently, that the set $\mathcal{D}_t$ is forward invariant.

V. Formation control of cooperative thrust-propelled UAVs with output constraints

We assert above that systems in strict feedback form (1) cover many models of physical systems, the most obvious instance being that of fully feedback-linearizable (hence fully-actuated) systems, such as second-order Lagrangian systems with n degrees of freedom and n control inputs. In this section we solve a problem of robust consensus for multi-agent constrained 3rd-order systems, which has relevance in certain robotics applications.

The case-study consists in designing robust distributed controllers to solve the position-consensus-based formation of multiple thrust-propelled UAVs under a set of realistic assumptions. It is assumed that the drones are equipped with relative-measurement sensors, so the graph representing the interaction between the agents is directed (either a directed spanning tree of a directed cycle). Furthermore, we assume that the system is subject to inter-agent constraints of the form (3). These constraints come, for one part from the embedded measurements devices, which are reliable only if used within a limited range. Hence, in order to maintain the connectivity of the graph, the UAVs must remain within a limited distance from their neighbors. On the other hand, in order to guarantee the safety of the systems, inter-agent collision avoidance must also be ensured. Finally, we assume that the agents are subject to bounded time-varying disturbances generated, e.g., by wind gusts, aerodynamic effects or unmodeled dynamics, which are common in applications involving cooperative UAVs.

In the following we present the model and the mathematical formulation of the problem at hand. We emphasize that the dynamic model of a UAV does not, a priori, fit in the class of systems characterized by Eq. (1), but we show that using a preliminary control loop it may be transformed into one with relative degree $\rho = 3$. The implementation of such controller, however, imposes the incorporation of saturations to the control method described in Section III-B. Thus, this meaningful case-study shows both the applicability and the versatility of our framework. Its efficacy is illustrated via brief numerical simulations.

A. UAV's model and problem formulation

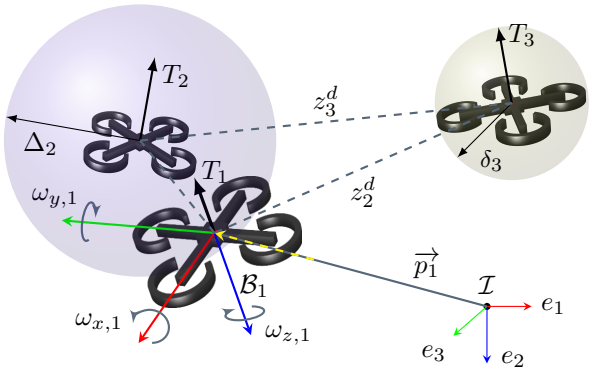

Fig. 2: Group of thrust propelled vehicles and Inertial frame

We consider a swarm of N UAVs as illustrated in Fig. 2; each vehicle's motion being described by a so-called "mixed" model that consists in a second-order Cartesian dynamics equation on E(3) and a first-order attitude kinematics equation on SO(3) —see, e.g., [15], [58], and [59]. This *underactuated* model describes some commercial UAVs, which accept only thrust and angular rates as the control inputs. It is also well-suited for control design and analysis since, in view of the fully-actuated and passive nature of the attitude dynamics, angular torques can be easily defined in order to track the designed angular rates.

The model for the ith agent is given by the equations

$$\dot{p}_i = v_i \tag{55a}$$

$$\dot{v}_i = -\frac{T_i}{m_i}\mathfrak{R}_i e_3 + g e_3 + \theta_{i,2}(t) \tag{55b}$$

$$\dot{\mathfrak{R}}_i = \mathfrak{R}_i S(\omega_i), \tag{56}$$

where m_i is the mass of the quadrotor, $e_3 = [0\ 0\ 1]^\top$ is the unitary vector in the vertical direction of the inertial frame $\mathcal{I}$, $p_i \in \mathbb{R}^3$ and $v_i \in \mathbb{R}^3$ are respectively the inertial position and inertial velocity, $\mathfrak{R}_i \in \mathrm{SO}(3)$ is the rotation matrix of the body-fixed frame $\mathcal{B}_i$ with respect to $\mathcal{I}$, g is gravity acceleration, and $\theta_{i,2} : \mathbb{R}_{\geq 0} \to \mathbb{R}^3$ is an essentially bounded disturbance. The inputs are the thrust force produced by the propellers, $T_i \in \mathbb{R}$, and the angular rate of the vehicle $\omega_i \in \mathbb{R}^3$ in the body-fixed frame $\mathcal{B}_i$ —see Figure 2 for an illustration.

The control goal is for the robots to achieve a predetermined formation in the three-dimensional space, centered at a point of non-predefined coordinates. More precisely, let the output of the multi-agent system be the relative position between pairs of connected agents. That is, in the way of (4)-(5), the edge states and error-edge states are defined as

$$z := [E^\top \otimes I_3]p \tag{57}$$

and

$$\tilde{z} = [E^\top \otimes I_3]p - z^d, \tag{58}$$

respectively, where $p^\top = [p_1^\top \ \cdots \ p_N^\top] \in \mathbb{R}^{3N}$ and $z^{d\top} = [z_1^{d\top} \ \cdots \ z_M^{d\top}] \in \mathbb{R}^{3M}$ are the relative displacements of the desired formation. Therefore, the control objective is that

$$\lim_{t\to\infty} \tilde{z}_k(t) = 0 \quad \forall k \leq M \tag{59a}$$

$$\lim_{t\to\infty} v_i(t) = 0 \quad \forall i \leq N. \tag{59b}$$

Now, in accordance to the realistic setting described previously, it is assumed that the robots are equipped solely with relative-measurements sensors. On one hand, this naturally leads to considering directed-topology graphs. Only directed-spanning-tree and directed-cycle topologies are considered but, alluding to Remark 4, we stress that the following results also apply to connected undirected graphs. On the other hand, the sensors are reliable only if "neighboring" agents remain within a certain range and, in order to guarantee the safety of the systems, these must also avoid collisions with one another.

Let Δ_k denote the maximal distance between the nodes i and j, such that the node j has access to information from the node i through the arc $e_k = (i, j)$. Similarly, let δ_k denote the minimal distance among neighbors such that collisions are avoided. Then, the connectivity and collision-avoidance constraints are encoded by the constraints set given in (3).

We also stress that the UAV model (55)-(56) is a nonlinear underactuated system. Indeed, the UAVs have six degrees of freedom (three-dimensional displacements and three rotations), but only four dimensions can be directly actuated using the actual inputs T_i and ω_i. To address this difficulty, some hierarchical approaches have been reported in the literature, using the natural cascaded structure of the UAVs' dynamics [15], [59]–[61]. Such designs have been used to solve the formation problem of swarms of UAVs interconnected through undirected and directed communication topologies —cf. [59], [60], [62]–[65]. Nonetheless, none of these works address the problem under inter-agent constraints, as stated next.

Robust formation problem with output constraints: Consider a multi-agent system composed of N quadrotor UAVs with underactuated dynamics described by (55)-(56). Let the interactions of the vehicles be modeled by a connected undirected graph, a directed spanning tree or a directed cycle. Moreover, let the output inter-agent constraints be given by the set (3). Find distributed controllers T_i and ω_i, $i \leq N$, that, in the absence of disturbances, that is, with $\theta_{i,2} \equiv 0$ for all $i \leq N$, achieve the objective (59) and render the constraints set (3) forward invariant, i.e., $z(0) \in \mathcal{D}$ implies that $z(t) \in \mathcal{D}$ for all $t \geq 0$. Furthermore, in the presence of disturbances, that is $\theta_{i,2} \not\equiv 0$, the control law must render the formation practically input-to-state stable with respect to the disturbances and the set $\mathcal{D}$ in (3) forward invariant. •

In the following, we present the control approach that solves the robust formation problem with output constraints. It is based on a change of variables, inspired by the hierarchical backstepping approach of [59], that allows us to consider the underactuated system (55)-(56) as a system in the form (1) with $\rho = 3$. Then, a slightly modified version of the controller designed in Section III-B may be used in order to obtain the desired formation under the connectivity and collision-avoidance constraints and with the desired robustness properties.

B. Control approach

The control architecture follows a hierarchical approach that exploits the natural cascaded interconnection between the translational dynamics (55) and the rotational kinematics, (56) —see Fig. 3. The design builds on the method proposed in the previous sections, but we must start by applying an implementable feedback transformation to represent the system (55) in the form (1). To that end, first note that (55) may be assimilated to a second-order integrator

$$\dot{p}_i = v_i \tag{60a}$$
$$\dot{v}_i = \zeta_i + \theta_{i,2}, \tag{60b}$$

with

$$\zeta_i := -\frac{T_i}{m_i}\mathfrak{R}_i e_3 + g e_3. \tag{61}$$

Nonetheless, the implementation of a virtual controller for (60), through the input ζ_i, is subject to the possibility of solving (61) for T_i, which is the actual control input. Because of the underactuation of (55), however, this is far from acquired. Indeed, note from (61) that the virtual input $\zeta_i \in \mathbb{R}^3$ cannot take an arbitrary value since $T_i \in \mathbb{R}$ and its direction are determined by the vehicle's orientation, $\mathfrak{R}_i$. In order to overcome the underactuation, we solve equation (61) dynamically, inspired by the distributed-backstepping approach in [59]. More precisely, we design the angular rates ω_i and an update law for the thrust T_i, so that ζ_i in (61) satisfies the dynamic equation

$$\dot{\zeta}_i = u_i, \quad i \leq N, \tag{62}$$

where $u_i \in \mathbb{R}^3$ is a new input. Note that now the system defined by (60) and (62) has the form (1) with $\rho = 3$. Hence, in the sequel, in (62), u_i is assumed to correspond to an output-constrained consensus control law designed as per the framework described in Section III.

Differentiating (61) with respect to time, and using (56), the left-hand side of (62) becomes

$$-\frac{\dot{T}_i}{m_i}\mathfrak{R}_i e_3 - \frac{T_i}{m_i}\mathfrak{R}_i S(\omega_i) e_3 = u_i. \tag{63}$$

Then, for a given u_i, we define $\nu_i \in \mathbb{R}^3$ as

$$\nu_i := u_i - \frac{c_3}{m_i} T_i \mathfrak{R}_i e_3, \tag{64}$$

where c_3 is a positive control gain. Next, replacing (64) into (63), we obtain

$$-\frac{1}{m_i}\left[\dot{T}_i\mathfrak{R}_i + T_i\mathfrak{R}_i S(\omega_i)\right] e_3 = \nu_i + \frac{c_3}{m_i} T_i \mathfrak{R}_i e_3$$

$$\iff \left[(\dot{T}_i + c_3\, T_i)\mathfrak{R}_i + T_i\mathfrak{R}_i S(\omega_i)\right] e_3 = -m_i\nu_i. \tag{65}$$

Left-multiplying by (the full-rank rotation matrix) $\mathfrak{R}_i^\top$, we see that the dynamic equation (65) is equivalent to

$$\left[T_i\omega_{yi},\ -T_i\omega_{xi},\ \dot{T}_i + c_3\, T_i\right]^\top = -m_i\mathfrak{R}_i^\top\nu_i. \tag{66}$$

Now let $\tilde{\nu}_i := [\tilde{\nu}_{i,x}\ \tilde{\nu}_{i,y}\ \tilde{\nu}_{i,z}]^\top = \mathfrak{R}_i^\top\nu_i$. Then, (66) holds if the angular rates are set to

$$\omega_i = \begin{bmatrix} \dfrac{m_i\tilde{\nu}_{i,y}}{T_i} & -\dfrac{m_i\tilde{\nu}_{i,x}}{T_i} & \omega_{zi} \end{bmatrix}^\top, \tag{67}$$

and the thrust is given by the update law

$$\dot{T}_i = -c_3\, T_i - m_i\tilde{\nu}_{i,z}. \tag{68}$$

Remark 7: Note that by transforming the UAV model (55) using (61)-(62), only the three translational dimensions are directly controlled. Therefore, only three of the four available inputs are needed to solve the formation problem. Indeed, note that from equation (66), the yaw component of the angular rate ω_{zi} is not needed for the control. Hence it may be considered as an additional degree of freedom and may be designed so that the vehicle follows a desired yaw trajectory. •

Thus, applying the previous transformation, the underactuated system (55) may be rewritten in the form (1), as desired, that is,

$$\dot{p}_i = v_i \tag{69a}$$
$$\dot{v}_i = \zeta_i + \theta_i \tag{69b}$$
$$\dot{\zeta}_i = u_i. \tag{69c}$$

Furthermore, denoting $v^\top = [v_1^\top\ \cdots\ v_N^\top] \in \mathbb{R}^{3N}$ and $\zeta^\top = [\zeta_1^\top\ \cdots\ \zeta_N^\top] \in \mathbb{R}^{3N}$, and using the edge transformation (58), the multi-agent system in the reduced error-edge coordinates becomes

$$\dot{\tilde{z}}_t = \left[E_t^\top \otimes I_3\right] v \tag{70a}$$
$$\dot{v} = \zeta + \theta_2 \tag{70b}$$
$$\dot{\zeta} = u. \tag{70c}$$

The transformed system (70) is in the form of (12) with $\rho = 3$. To apply the robust control law (23), designed in the previous section for the constrained-consensus problem of high-order systems, we define the backstepping error variables

$$\tilde{v} = v - v_f \quad \text{and} \quad \tilde{\zeta} = \zeta - \zeta_f. \tag{71}$$

The filtered signals v_f and ζ_f are the outputs of command filters given in (19), with inputs v^* and ζ^*, respectively, corresponding to the desired virtual controllers given by

$$v^* := -c_1[E_\odot \otimes I_3]\nabla W(\tilde{z}) \tag{72}$$

and

$$\zeta^* := -c_2\tilde{v} + \omega_n\alpha_{1,2}, \tag{73}$$

where $\nabla W(\tilde{z})$ is the gradient of the barrier Lyapunov function defined in (15) and (13) with the weight recentered barrier

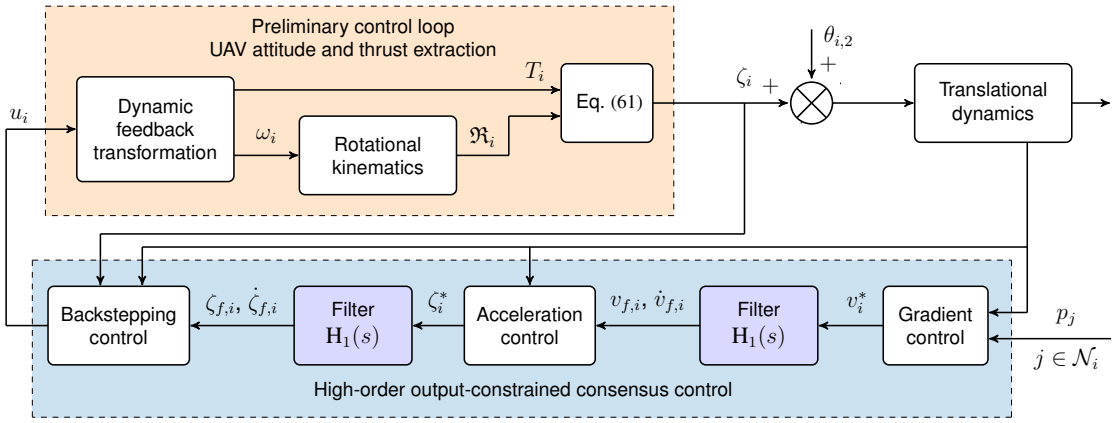

Fig. 3: Block diagram of the hierarchical control approach.

function given by

$$B_k(z_k) = \kappa_{1,k}\left[\ln\left(\frac{\Delta_k^2}{\Delta_k^2-|z_k|^2}\right)-\ln\left(\frac{\Delta_k^2}{\Delta_k^2-|z_k^d|^2}\right)\right] + \kappa_{2,k}\left[\ln\left(\frac{|z_k|^2}{|z_k|^2-\delta_k^2}\right)-\ln\left(\frac{|z_k^d|^2}{|z_k^d|^2-\delta_k^2}\right)\right], \tag{74}$$

$$\kappa_{1,k} := \frac{\delta_k^2}{|z_k^d|^2(|z_k^d|^2-\delta_k^2)}, \quad \kappa_{2,k} := \frac{1}{\Delta_k^2-|z_k^d|^2}. \tag{75}$$

This function and its gradient are equal to zero at the desired formation configuration, i.e., $B_k(z_k^d) = 0$, $\nabla B_k(z_k^d) = 0$. Moreover it directly encodes the constraints in terms of the original edge-state z_k, i.e., $B_k(z_k) \to \infty$ as either $|z_k| \to \Delta_k$ or $|z_k| \to \delta_k$ —see Remark 2.

Then, akin to (23), the new input u is given by

$$u := -c_3\tilde{\zeta} + \omega_n\alpha_{2,2} - \tilde{v}. \tag{76}$$

After the developments in Section III and Theorem 1, the transformed controller (76), with (72)-(73) and (19), solves the robust formation problem with output constraints for system (69). However, a closer inspection shows that there is one more technical difficulty to circumvent. Note that, from (67), the dynamic solution to the equation (61) is valid if and only if $T_i \neq 0$. In order to address this additional constraint, we perform a control redesign which respects the control method and the stability analysis in Sections III-B and IV.

Note that, from (61), the condition $T_i \neq 0$ is satisfied if the desired virtual control ζ_i^* satisfies $\zeta_i^* \neq ge_3$, for all $i \leq N$. Therefore, the virtual control input ζ^* is modified to

$$\zeta^* := \mathrm{sat}\left(-c_2\tilde{v} + \omega_n\alpha_{1,2}\right), \tag{77}$$

where $\mathrm{sat}(\cdot)$ is a saturation function $\mathbb{R}^N \to \mathbb{R}^N$ defined element-wise, i.e., $\mathrm{sat}(s) = \left[\sigma(s_1)^\top \cdots \sigma(s_N)^\top\right]^\top$, where, e.g., $\sigma(s_i) = \mathrm{sign}(s_i)\min\{|s_i|, \bar{\zeta}_M\}$, with $\bar{\zeta}_M < g$, or any other odd monotonic function, bounded in absolute value.

Then, we have the following.

Proposition 1: For almost any initial conditions satisfying $z(0) \in \mathcal{D}$, except for a set of measure zero, there exists ϵ^*, such that, for $\epsilon \in (0, \epsilon^*]$ where $\epsilon := 1/\omega_n$, the control law (67)-(68) and (76), with (19), (72) and (77), solves the robust formation problem with output constraints for system (55). □

Proof: The proof follows the same arguments as the proof of Theorem 1. First, following the same arguments used in Section IV-A, the system (70) in closed-loop with (76) may be written in singular-perturbation form

$$\dot{\tilde{z}}_t = -c_1[E_t^\top E_\odot \otimes I_n]\nabla W(\tilde{z}) + [E_t^\top \otimes I_n]\left[\tilde{v} + \tilde{\alpha}_{1,1}\right] \tag{78a}$$

$$\dot{\tilde{v}} = -\mathrm{sat}(-c_2\tilde{v} + \omega_n\tilde{\alpha}_{1,2}) + \tilde{\zeta} + \tilde{\alpha}_{2,1} - \omega_n\tilde{\alpha}_{1,2} + \theta_2 \tag{78b}$$

$$\dot{\tilde{\zeta}} = -c_3\,\tilde{\zeta} - \tilde{v} \tag{78c}$$

$$\epsilon\dot{\tilde{\alpha}} = \tilde{A}\tilde{\alpha} - \epsilon\frac{\partial h(\xi)}{\partial \xi}\dot{\xi}, \quad \xi^\top = \begin{bmatrix}\tilde{z}_t^\top & \tilde{v}^\top & \tilde{\zeta}^\top\end{bmatrix}. \tag{78d}$$

Now, proceeding as in Section IV-B, in order to apply the singular-perturbation result for multi-stable systems derived in [35, Theorem 2], we need to show that the boundary layer system is asymptotically stable and that the reduced slow system is input-to-state stable with respect to the set $\mathcal{W}\times\{0\}^2$ and input $\theta_{i,2}$, $i \leq N$.

Since $\tilde{A}$ is Hurwitz, the origin for the boundary-layer system (41) is exponentially stable. Now consider the reduced system

$$\dot{\tilde{z}}_t = -c_1[E_t^\top E_\odot \otimes I_n]\nabla W(\tilde{z}) + [E_t^\top \otimes I_n]\tilde{v} \tag{79a}$$

$$\dot{\tilde{v}} = -\mathrm{sat}(c_2\tilde{v}) + \tilde{\zeta} + \theta_2 \tag{79b}$$

$$\dot{\tilde{\zeta}} = -c_3\,\tilde{\zeta} - \tilde{v}. \tag{79c}$$

From (52) the subsystem (79a) is input-to-state stable with respect to the set $\mathcal{W}$ and to the input $\tilde{v}$. Next, consider the subsystem (79b)-(79c). Let $\varepsilon_u \in (0,1)$ and define the Lyapunov function

$$V_2(\tilde{v},\tilde{\zeta}) = \frac{(1+c_3\,\varepsilon_u)}{2}|\tilde{v}|^2 + \frac{1}{2}|\tilde{\zeta}|^2 + \varepsilon_u\,\tilde{\zeta}^\top\tilde{v}, \tag{80}$$

which is positive definite. Its derivative along (79b)-(79c) satisfies

$$\dot{V}_2(\tilde{v},\tilde{\zeta}) \leq -(1+\varepsilon_u c_3 - \gamma_v)|\tilde{v}|\mathrm{sat}(c_2|\tilde{v}|) - \left(c_3 - \varepsilon_u - \frac{\varepsilon_u^2}{1+c_3\,\varepsilon_u}\right)|\tilde{\zeta}|^2 + \frac{2\varepsilon_u}{1+c_3\,\varepsilon_u}|\theta|^2. \tag{81}$$

Hence, choosing $\gamma_v > 0$ and $\varepsilon_u > 0$ small enough so that

$$\gamma_2 := c_3 - \varepsilon_u - \frac{\varepsilon_u^2}{1+c_3\,\varepsilon_u} > 0$$

and $\gamma_1 := 1 + \varepsilon_u c_3 - \gamma_v > 0$, we have

$$\dot{V}_2(\tilde{v}, \tilde{\zeta}) \leq -\gamma_1 |\tilde{v}| \text{sat}(c_2|\tilde{v}|) - \gamma_2 |\tilde{\zeta}|^2 + \gamma_3 |\theta_2|^2 \qquad (82)$$

where $\gamma_3 := 2\varepsilon_u/(1 + c_3\,\varepsilon_u)$. The inequality (82) implies input-to-state stability of (79b)-(79c) with respect to the origin and to θ_2. Using [36, Theorem 3.1] we conclude that, for all initial conditions $\xi(0)$ such that $z_t(0) \in \mathcal{D}_t$ and all essentially bounded inputs θ_2, the reduced system (79) is input-to-state stable with respect to $\mathcal{W}_\Theta := \mathcal{W} \times \{0\}^2$ and to the input θ_2. Furthermore, $\mathcal{W}_\Theta$ qualifies as a $\mathcal{W}$-limit set for (79).

Now, since the boundary layer system is exponentially stable and the reduced system is input-to-state stable with respect to $\mathcal{W}_\Theta$ and θ_2, using Theorem 1, we conclude that the controller (76), with (19), (72), and (77) solves the robust consensus problem with output constraints for system (70). This, in turn, implies that the actual controllers (67)-(68) solve the robust formation problem with output constraints for multi-agent system (55). ■

C. Simulation results

In this section we illustrate the performance of the controller (67)–(68) via a numerical example consisting in the rendezvous of six UAVs, subject to inter-agent collision avoidance and connectivity restrictions. It is assumed that the measurement range of each agent is different and that they are equipped with proximity sensors. Under these conditions, it is natural to model the network using a directed topology as in Fig. 4. It is assumed, however, that only at the initial time the vehicles are interconnected, so the controller must preserve such connectivity.

The initial conditions and constraint parameters are presented in Table I. The desired formation corresponds to a hexagon and is determined by the desired relative position vector $z_{dk} = (z_{dk,x}, z_{dk,y}, z_{dk,z})$, for each $k \leq 5$, set to $(1, 0.5, 0)$, $(-1, 1.5, 0)$, $(-1, 0.5, 0)$, $(-2, 1, 0)$, $(-1, 0.5, 0)$.

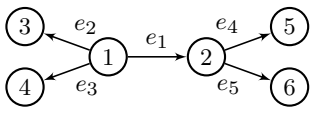

Fig. 4: Interaction topology: directed spanning tree

The saturation limit for the desired controller of the translational dynamics was set to $\bar{\zeta}_M = 7$ m/s^2, the controller gains to $c_1 = 1$, $c_2 = 0.8$, $c_3 = 3$, and the filter natural frequency to $\omega_n = 350$ rad/s. We consider the mass of each drone to be $m_i = 0.4$ kg.

TABLE I: Initial conditions and constraint parameters

Index	p_x	p_y	p_z	v_x	v_y	v_z	Δ_k	δ_k
1	2.4	0	-1	0.6	-0.8	0	2.5	0.2
2	-0.58	-0.9	0	-0.3	0	0	3.4	0.2
3	4	1.8	0	1.1	0.3	0	3.8	0.2
4	5	-2	0	0.1	0	0	3.5	0.2
5	-4.2	-0.45	0	0	0	0	3.7	0.2
6	-2	-4.2	2	-0.8	0	0	4.2	0.2

It is also assumed that the UAVs are subject to a disturbance modeled as a smoothed vanishing step, that is,

$$\theta_i(t) = -\,\sigma_i(t)\,[1\ 1\ 0]^\top$$

$$\sigma_i(t) = \begin{cases} -0.6\big[\tanh(2(t-15)) - 1\big] & \text{if} \quad i \in \{3, 5\} \\ 0.6\big[\tanh(2(t-15)) - 1\big] & \text{if} \quad i = 2 \\ 0 & \text{if} \quad i \in \{1, 4, 6\}. \end{cases}$$

In Fig. 5 are illustrated the paths of each agent as well as the final desired formation for the multi-agent system. In Fig. 6 are presented the trajectories of the inter-agent distances. As can be seen from the figure, both connectivity and collision avoidance constraints (dashed lines) are always respected, even in the presence of the disturbance. Furthermore, as soon as the disturbance vanishes after 15 seconds, the agents converge to the desired static formation.

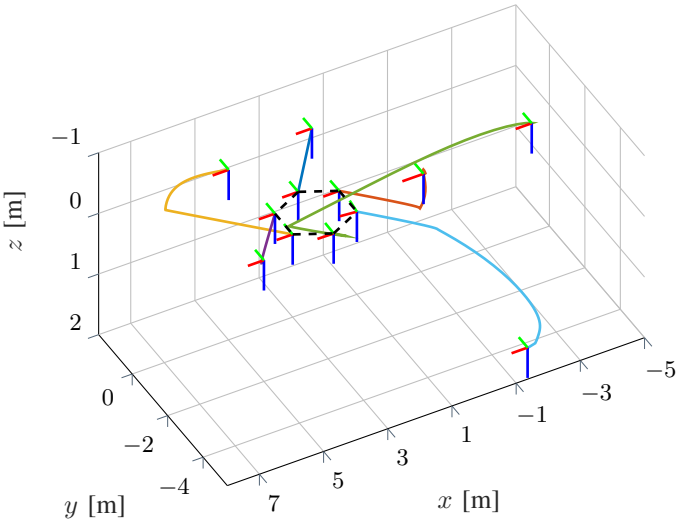

Fig. 5: Paths of the agents.

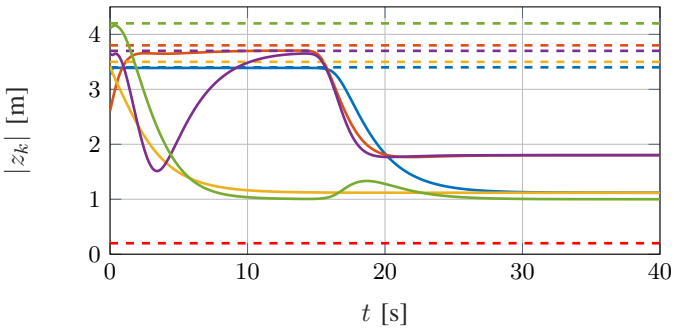

Fig. 6: Distances between neighbor UAVs. The dashed lines represent the connectivity and collision avoidance constraints.

VI. Conclusions

We presented a control framework of broad applicability to solve the consensus problem for systems of high relative degree in feedback form, subject to inter-agent constraints. The design is based on the gradient of barrier Lyapunov functions and on the command filtered backstepping approach. From a theoretical viewpoint, it is important to emphasize that

beyond mere convergence to the consensus manifold, we also established robustness in the sense of practical input-to-state multi-stability with respect to external disturbances. Moreover, our results hold for both undirected and directed graphs.

Furthermore, we showed that our control framework is versatile in that it serves as basis for consensus control design of systems that are not, a priori, in the assumed strict-feedback form. In particular, we solved the rendezvous (open) problem for a group of UAVs subject to connectivity and inter-agent collision-avoidance constraints. From a control-practice viewpoint, it is remarked that each agent's control input requires only its own velocity and orientation, as well as the relative position of its neighbors. In that light, we believe that our theoretical results may pave the way for solving other consensus-based problems in realistic settings for different types of dynamical systems. Current research focuses on solving the consensus-tracking problem with limited measurements and the generalization of our main theoretical statements to multiagent systems interconnected over arbitrary directed graphs (containing an underlying spanning tree).

APPENDIX I
CRITICAL POINTS OF THE BARRIER LYAPUNOV FUNCTION

First note that the gradient of the barrier Lyapunov function (13) with (74) may be written as

$$\nabla W_k(\tilde{z}_k) := \frac{\partial W_k(\tilde{z}_k)}{\partial \tilde{z}_k} = \varrho_k(\tilde{z}_k + z_k^d)\left[\tilde{z}_k + z_k^d\right] - z_k^d, \quad (83)$$

where

$$\varrho_k(s_k) = 1 + \frac{\kappa_{1,k}}{\Delta_k^2 - |s_k|^2} - \frac{\kappa_{2,k}\delta_k^2}{|s_k|^2(|s_k|^2 - \delta_k^2)}. \quad (84)$$

Then the Hessian of the barrier Lyapunov function reads

$$\begin{aligned}\mathcal{H}_k(\tilde{z}_k) :=& \frac{\partial}{\partial \tilde{z}_k}\Big[\nabla W_k(\tilde{z}_k)\Big] \\ =& \varrho_k(\tilde{z}_k + z_k^d) I_N + 2\tilde{\varrho}_k(\tilde{z}_k + z_k^d)\left[\tilde{z}_k + z_k^d\right]\left[\tilde{z}_k + z_k^d\right]^\top \end{aligned} \quad (85)$$

where

$$\tilde{\varrho}_k(s_k) := \frac{\kappa_{1,k}}{\left(\Delta_k^2 - |s_k|^2\right)^2} + \frac{\kappa_{2,k}}{\left(|s_k|^2 - \delta_k^2\right)^2} - \frac{\kappa_{2,k}}{|s_k|^4}. \quad (86)$$

From a straightforward computation, we see that the eigenvalues of $\mathcal{H}_k(\tilde{z}_k)$ are

$$\lambda_{i,k}(\tilde{z}_k) = \varrho_k(\tilde{z}_k + z_k^d), \quad i \in \{1, \dots, n-1\} \quad (87a)$$

$$\lambda_{n,k}(\tilde{z}_k) = \varrho_k(\tilde{z}_k + z_k^d) + 2\tilde{\varrho}_k(\tilde{z}_k + z_k^d)|\tilde{z}_k + z_k^d|^2. \quad (87b)$$

To show that $\tilde{z}_k^*$ is a saddle point it suffices to prove that at least one of these eigenvalues is negative. From (84), (86), and (75), it follows that for all $\delta_k < |\tilde{z}_k + z_k^d| < \Delta_k$,

$$\begin{aligned}\varrho_k(s_k) + 2\tilde{\varrho}_k(s_k)|s_k|^2 =& 1 + \frac{\kappa_{1,k}(\Delta_k^2 + |s_k|^2)}{(\Delta_k^2 - |s_k|^2)^2} \\ &+ \frac{\kappa_{2,k}\delta_k^2(3|s_k|^2 - \delta_k^2)}{|s_k|^2(|s_k|^2 - \delta_k^2)^2} > 1.\end{aligned} \quad (88)$$

Hence, we show that $\lambda_{i,k}(\tilde{z}_k^*) = \varrho_k(\tilde{z}_k^* + z_k^d) < 0$. To that end, note that from (83), since $\tilde{z}_k^*$ is a singular point of W_k,

$$\varrho_k(\tilde{z}_k^* + z_k^d)\left[\tilde{z}_k^* + z_k^d\right] = z_k^d. \quad (89)$$

Now, since $\delta_k < |\tilde{z}_k^* + z_k^d| < \Delta_k$, we have $\left[\tilde{z}_k^* + z_k^d\right] \neq 0$. Also, $z_k^d \neq 0$. Therefore, $\varrho_k(\tilde{z}_k^* + z_k^d) \neq 0$. It follows that $\left[\tilde{z}_k^* + z_k^d\right] =: z_k^*$, which is the critical point expressed in the original relative-position coordinates, is aligned with z_k^d. Furthermore, for each $k \leq M$ the barrier-Lyapunov function W_k may possess only two singular points belonging to $\{z_k \in \mathbb{R}^n : \delta_k < |z_k| < \Delta_k\}$, but these must have opposite sign. Consequently, there exists $a > 0$ such that $z_k^* = -a\, z_k^d$ or, equivalently,

$$\varrho_k(z_k^*) = -\frac{1}{a} < 0, \quad (90)$$

as required.

On the other hand, we have from (84) that $\varrho_k(z_k^d) = 1$, so from (87), we can conclude that z_k^d is a minimum.

APPENDIX II
STABILITY OF MULTIPLE INVARIANT SETS

Terminology: A function $\gamma : \mathbb{R}_{\geq 0} \to \mathbb{R}_{\geq 0}$ is said to be of class $\mathcal{K}$, if it is continuous, strictly increasing and zero at zero. If moreover $\gamma(s) \to \infty$ as $s \to \infty$, we say that $\gamma \in \mathcal{K}_\infty$. A function $\beta : \mathbb{R}_{\geq 0} \times \mathbb{R}_{\geq 0} \mapsto \mathbb{R}_{\geq 0}$ is said to be of class $\mathcal{KL}$ if, for each fixed t, the function $\beta(\cdot, t)$ is of class $\mathcal{K}$ and for each fixed s, the function $\beta(s, \cdot)$ is non-decreasing and tends to zero as $t \to \infty$.

The following results on practical input-to-state stability of multi-stable systems is adapted from [35, Theorem 2] to the notation used in this paper.

Theorem 3: Consider a singularly perturbed system of the form (38). Assume that:

1) the reduced system (39) is input-to-state stable with respect to an acyclic $\mathcal{W}$-limit set $\mathcal{W}_\Theta$ and an input θ;
2) the equilibrium $\tilde{\alpha} = 0$ of the boundary layer system (41) is globally asymptotically stable.

Then, there exist a class $\mathcal{KL}$ function β_α and a class $\mathcal{K}_\infty$ function η_θ and, for any pair d_1, $d_2 > 0$, there exists an $\epsilon^* > 0$ such that, for any $\epsilon \in (0, \epsilon^*]$, any essentially bounded function $\theta(t)$, and any initial condition $\xi(0) \in \mathcal{D}_t \times \mathbb{R}^{nN(\rho-1)}$, and $\max\{|\xi(0)|_{\mathcal{W}_\Theta}, |\tilde{\alpha}(0)|, \|\theta\|_\infty, \|\dot{\theta}\|_\infty\} \leq d_1$, it holds that

$$\limsup_{t \to +\infty} |\xi(t)|_{\mathcal{W}_\Theta} \leq \eta_\theta(\|\theta\|_\infty) + d_2 \quad (91a)$$

$$|\tilde{\alpha}(t)| \leq \beta_\alpha\left(|\tilde{\alpha}(0)|, \frac{t}{\epsilon}\right) + d_2. \quad \forall t \geq 0 \quad (91b)$$

□

For completeness we include the following elements on input-to-state multi-stability adapted, respectively, from [36, Definition 2.7] and [36, Theorem 2.8].

Definition 2: A $\mathcal{C}^1$ function $V : \mathcal{M} \to \mathbb{R}_{\geq 0}$ is a practical ISS-Lyapunov function for a system $\dot{x} = f(x, \theta)$ if there exist $\mathcal{K}_\infty$ functions η_1, η, γ and $q \geq 0$ such that, for all $x \in \mathcal{M}$ and all θ, the following holds:

$$\begin{aligned}\eta_1(|x|_{\mathcal{W}}) \leq& V(x) \\ \nabla V(x)^\top f(x, \theta) \leq& -\eta(|x|_{\mathcal{W}}) + \gamma(|\theta|) + q.\end{aligned} \quad (92)$$

If (92) holds with $q = 0$, then V is said to be an ISS-Lyapunov function. □

Theorem 4: Consider a system $\dot{x} = f(x, \theta)$ and an acyclic $\mathcal{W}$-limit set $\mathcal{W}$. Then, system $\dot{x} = f(x, \theta)$ is input-to-state stable with respect to input θ and to the set $\mathcal{W}$ if and only if it admits an ISS-Lyapunov function. □

REFERENCES

[1] W. Ren and R. Beard, *Distributed Consensus in Multi-vehicle Cooperative Control: Theory and Applications*, 1st ed. Springer Publishing Company, Incorporated, 2010.

[2] Y. Guo, *Distributed cooperative control: emerging applications*. John Wiley & Sons, 2017.

[3] S. Zhao, "Affine formation maneuver control of multiagent systems," *IEEE Transactions on Automatic Control*, vol. 63, no. 12, pp. 4140–4155, 2018.

[4] F. Chen, W. Ren *et al.*, "On the control of multi-agent systems: A survey," *Foundations and Trends® in Systems and Control*, vol. 6, no. 4, pp. 339–499, 2019.

[5] R. Olfati-Saber, J. A. Fax, and R. M. Murray, "Consensus and cooperation in networked multi-agent systems," *Proc. IEEE*, vol. 95, no. 1, pp. 215–233, Jan. 2007.

[6] D. Mukherjee and D. Zelazo, "Robustness of consensus over weighted digraphs," *IEEE Transactions on Network Science and Engineering*, 2018.

[7] A. Dong and J. A. Farrell, "Cooperative control of multiple nonholonomic mobile agents," *IEEE Transactions on Automat. Contr.*, vol. 53, no. 6, pp. 1434–1447, 2008.

[8] C. P. Bechlioulis and K. J. Kyriakopoulos, "Robust model-free formation control with prescribed performance and connectivity maintenance for nonlinear multi-agent systems," in *53rd IEEE Conference on Decision and Control*, 2014, pp. 4509–4514.

[9] A. Nikou, C. K. Verginis, and D. V. Dimarogonas, "Robust distance-based formation control of multiple rigid bodies with orientation alignment," *IFAC-PapersOnLine*, vol. 50, no. 1, pp. 15 458 – 15 463, 2017, 20th IFAC World Congress.

[10] X. Wang, G. Wang, S. Li, and K. Lu, "Composite sliding-mode consensus algorithms for higher-order multi-agent systems subject to disturbances," *IET Control Theory & Applications*, vol. 14, no. 2, pp. 291–303, 2019.

[11] C.-C. Hua, K. Li, and X.-P. Guan, "Leader-following output consensus for high-order nonlinear multiagent systems," *IEEE Transactions on Automatic Control*, vol. 64, no. 3, pp. 1156–1161, 2018.

[12] H. Rezaee and F. Abdollahi, "Average consensus over high-order multiagent systems," *IEEE Transactions on Automatic Control*, vol. 60, no. 11, pp. 3047–3052, 2015.

[13] Z. Zuo, B. Tian, M. Defoort, and Z. Ding, "Fixed-time consensus tracking for multiagent systems with high-order integrator dynamics," *IEEE Transactions on Automatic Control*, vol. 63, no. 2, pp. 563–570, 2017.

[14] M. Mesbahi and M. Egerstedt, *Graph theoretic methods in multiagent networks*, ser. Princeton series in applied mathematics. Princeton: Princeton University Press, 2010, oCLC: ocn466341412.

[15] M. Hua, T. Hamel, P. Morin, and C. Samson, "Introduction to feedback control of underactuated VTOL vehicles: A review of basic control design ideas and principles," *IEEE Control Systems Magazine*, vol. 33, no. 1, pp. 61–75, 2013.

[16] H. A. Poonawala and M. W. Spong, "Preserving strong connectivity in directed proximity graphs," *IEEE Transactions Automatic Control*, vol. 62, no. 9, pp. 4392–4404, Sep. 2017.

[17] M. Santilli, P. Mukherjee, A. Gasparri, and R. K. Williams, "Distributed connectivity maintenance in multi-agent systems with field of view interactions," in *2019 American Control Conference (ACC)*, 2019, pp. 766–771.

[18] Z. Zhou and X. Wang, "Constrained consensus in continuous-time multiagent systems under weighted graph," *IEEE Transactions on Automatic Control*, vol. 63, no. 6, pp. 1776–1783, 2017.

[19] Y. Shang, "Resilient consensus in multi-agent systems with state constraints," *Automatica*, vol. 122, p. 109288, 2020.

[20] H. Chu, D. Yue, C. Dou, and L. Chu, "Consensus of multiagent systems with time-varying input delay and relative state saturation constraints," *IEEE Transactions on Systems, Man, and Cybernetics: Systems*, 2020.

[21] E. Restrepo, A. Loría, I. Sarras, and J. Marzat, "Stability and robustness of edge-agreement-based consensus protocols for undirected proximity graphs," *International Journal of Control*, pp. 1–9, 2020.

[22] J. Liu, C. Wang, and Y. Xu, "Distributed adaptive output consensus tracking for high-order nonlinear time-varying multi-agent systems with output constraints and actuator faults," *Journal of the Franklin Institute*, vol. 357, no. 2, pp. 1090–1117, 2020.

[23] C. P. Bechlioulis and G. A. Rovithakis, "Decentralized robust synchronization of unknown high order nonlinear multi-agent systems with prescribed transient and steady state performance," *IEEE Transactions on Automatic Control*, vol. 62, no. 1, pp. 123–134, 2016.

[24] J. Fu, G. Wen, Y. Lv, and T. Huang, "Barrier function based consensus of high-order nonlinear multi-agent systems with state constraints," in *International Conference on Neural Information Processing*. Springer, 2019, pp. 492–503.

[25] J. Ghommam, L. F. Luque-Vega, and M. Saad, "Distance-based formation control for quadrotors with collision avoidance via lyapunov barrier functions," *International Journal of Aerospace Engineering*, 2020.

[26] Y. Zou and Z. Meng, "Distributed hierarchical control for multiple vertical takeoff and landing UAVs with a distance-based network topology," *International Journal of Robust and Nonlinear Control*, vol. 29, no. 9, pp. 2573–2588, 2019.

[27] C. K. Verginis, A. Nikou, and D. V. Dimarogonas, "Robust formation control in se(3) for tree-graph structures with prescribed transient and steady state performance," *Automatica*, vol. 103, pp. 538 – 548, 2019.

[28] C. P. Bechlioulis and G. A. Rovithakis, "Prescribed performance adaptive control for multi-input multi-output affine in the control nonlinear systems," *IEEE Transactions on Automatic Control*, vol. 55, no. 5, pp. 1220–1226, 2010.

[29] D. Zelazo, A. Rahmani, and M. Mesbahi, "Agreement via the edge Laplacian," in *46th IEEE Conference on Decision and Control*, New Orleans, LA, USA, 2007, pp. 2309–2314.

[30] J. A. Marshall, M. E. Broucke, and B. A. Francis, "Formations of vehicles in cyclic pursuit," *IEEE Transactions on Automatic Control*, vol. 49, no. 11, pp. 1963–1974, Nov 2004.

[31] K. P. Tee, S. S. Ge, and E. H. Tay, "Barrier Lyapunov functions for the control of output-constrained nonlinear systems," *Automatica*, vol. 45, no. 4, pp. 918–927, 2009.

[32] E. Rimon and D. E. Koditschek, "Exact robot navigation using artificial potential functions," *IEEE Transactions on Robotics and Automation*, vol. 8, no. 5, pp. 501–518, Oct. 1992.

[33] M. Krstic, P. V. Kokotovic, and I. Kanellakopoulos, *Nonlinear and adaptive control design*. John Wiley & Sons, Inc., 1995.

[34] J. A. Farrell, M. Polycarpou, M. Sharma, and W. Dong, "Command filtered backstepping," *IEEE Transactions on Automatic Control*, vol. 54, no. 6, pp. 1391–1395, 2009.

[35] P. Forni and D. Angeli, "Perturbation theory and singular perturbations for input-to-state multistable systems on manifolds," *IEEE Transactions on Automatic Control*, vol. 64, no. 9, pp. 3555–3570, 2018.

[36] ——, "Input-to-state stability for cascade systems with multiple invariant sets," *Systems & Control Letters*, vol. 98, pp. 97–110, 2016.

[37] Y.-H. Lim and H.-S. Ahn, "Consensus under saturation constraints in interconnection states," *IEEE Transactions on Automatic Control*, vol. 60, no. 11, pp. 3053–3058, 2015.

[38] D. H. Nguyen, T. Narikiyo, and M. Kawanishi, "Robust consensus analysis and design under relative state constraints or uncertainties," *IEEE Transactions Automatic Control*, vol. 63, no. 6, pp. 1784–1790, June 2018.

[39] V. T. Pham, N. Messai, D. H. Nguyen, and N. Manamanni, "Robust formation control under state constraints of multi-agent systems in clustered networks," *Systems & Control Letters*, vol. 140, p. 104689, 2020.

[40] G. Wang, C. Wang, and X. Cai, "Consensus control of output-constrained multiagent systems with unknown control directions under a directed graph," *International Journal of Robust and Nonlinear Control*, vol. 30, no. 5, pp. 1802–1818, 2020.

[41] T.-S. Li, D. Wang, G. Feng, and S.-C. Tong, "A DSC approach to robust adaptive NN tracking control for strict-feedback nonlinear systems," *IEEE transactions on systems, man, and cybernetics, part b (cybernetics)*, vol. 40, no. 3, pp. 915–927, 2009.

[42] B. Xu, D. Wang, Y. Zhang, and Z. Shi, "Dob-based neural control of flexible hypersonic flight vehicle considering wind effects," *IEEE Transactions on Industrial Electronics*, vol. 64, no. 11, pp. 8676–8685, 2017.

[43] H. Du, M. Z. Chen, and G. Wen, "Leader–following attitude consensus for spacecraft formation with rigid and flexible spacecraft," *Journal of Guidance, Control, and Dynamics*, vol. 39, no. 4, pp. 944–951, 2016.

[44] E. Nuño, D. Valle, I. Sarras, and L. Basañez, "Leader–follower and leaderless consensus in networks of flexible-joint manipulators," *European Journal of Control*, vol. 20, no. 5, pp. 249–258, 2014.

[45] G. Duan, "High-order fully actuated system approaches: Part ii. generalized strict-feedback systems," *International Journal of Systems Science*, pp. 1–18, 2020.
[46] H. K. Khalil, *Nonlinear systems; 2nd ed.* Upper Saddle River, NJ: Prentice-Hall, 1996.
[47] K. P. Tee and S. S. Ge, "Control of state-constrained nonlinear systems using integral barrier Lyapunov functionals," in *2012 IEEE 51st IEEE Conference on Decision and Control (CDC)*. IEEE, 2012, pp. 3239–3244.
[48] C. Feller and C. Ebenbauer, "Weight recentered barrier functions and smooth polytopic terminal set formulations for linear model predictive control," in *2015 American Control Conference (ACC)*. IEEE, 2015, pp. 1647–1652.
[49] D. Panagou, D. M. Stipanovic, and P. G. Voulgaris, "Distributed coordination control for multi-robot networks using Lyapunov-like barrier functions," *IEEE Transactions on Automat. Contr.*, vol. 61, no. 3, pp. 617–632, Mar. 2016.
[50] M. Ji and M. Egerstedt, "Distributed coordination control of multiagent systems while preserving connectedness," *IEEE Transactions Robot.*, vol. 23, no. 4, pp. 693–703, Aug. 2007.
[51] D. Boskos and D. V. Dimarogonas, "Robustness and invariance of connectivity maintenance control for multiagent systems," *SIAM J. on Control and Optimization*, vol. 55, no. 3, pp. 1887–1914, 2017.
[52] Z. Zeng, X. Wang, and Z. Zheng, "Nonlinear consensus under directed graph via the edge Laplacian," in *The 26th Chinese Control and Decision Conference (2014 CCDC)*. Changsha, China: IEEE, May 2014, pp. 881–886.
[53] E. Restrepo, A. Loría, I. Sarras, and J. Marzat, "Robust consensus and connectivity-maintenance under edge-agreement-based protocols for directed-spanning tree graph," in *21st IFAC World Congress*, 2020.
[54] W. Dong, J. A. Farrell, M. M. Polycarpou, V. Djapic, and M. Sharma, "Command filtered adaptive backstepping," *IEEE Transactions on Control Systems Technology*, vol. 20, no. 3, pp. 566–580, 2011.
[55] P. V. Kokotović and H. J. Sussmann, "A positive real condition for global stabilization of nonlinear systems," *Syst. & Contr. Letters*, vol. 13, no. 4, pp. 125–133, 1989.
[56] R. Sepulchre, M. Janković, and P. V. Kokotović, "Recursive designs and feedback passivation," in *Systems and control in the twenty-first century*. Springer, 1997, pp. 313–326.
[57] P. Monzón and R. Potrie, "Local and global aspects of almost global stability," in *Proceedings of the 45th IEEE Conference on Decision and Control*. IEEE, 2006, pp. 5120–5125.
[58] M. Hua, T. Hamel, P. Morin, and C. Samson, "A control approach for thrust-propelled underactuated vehicles and its application to vtol drones," *IEEE Transactions on Automatic Control*, vol. 54, no. 8, pp. 1837–1853, 2009.
[59] D. Lee, "Distributed backstepping control of multiple thrust-propelled vehicles on a balanced graph," *Automatica*, vol. 48, no. 11, pp. 2971 – 2977, 2012.
[60] A. Abdessameud, "Formation control of VTOL-UAVs under directed and dynamically-changing topologies," in *2019 American Control Conference (ACC)*, 2019, pp. 2042–2047.
[61] S. Bertrand, N. Gunard, T. Hamel, H. Piet-Lahanier, and L. Eck, "A hierarchical controller for miniature VTOL UAVs: Design and stability analysis using singular perturbation theory," *Control Engineering Practice*, vol. 19, no. 10, pp. 1099 – 1108, 2011.
[62] Y. Zou and Z. Meng, "Coordinated trajectory tracking of multiple vertical take-off and landing UAVs," *Automatica*, vol. 99, pp. 33 – 40, 2019.
[63] Y. Zou, Z. Zhou, X. Dong, and Z. Meng, "Distributed formation control for multiple vertical takeoff and landing UAVs with switching topologies," *IEEE/ASME Transactions on Mechatronics*, vol. 23, no. 4, pp. 1750–1761, 2018.
[64] A. Roza, M. Maggiore, and L. Scardovi, "Local and distributed rendezvous of underactuated rigid bodies," *IEEE Transactions on Automatic Control*, vol. 62, no. 8, pp. 3835–3847, 2017.
[65] H. Wang, "Second-order consensus of networked thrust-propelled vehicles on directed graphs," *IEEE Transactions on Automatic Control*, vol. 61, no. 1, pp. 222–227, 2016.

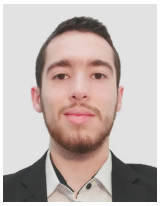

Esteban Restrepo obtained his BSc degree on Mechatronics engineering from Universidad EIA, Envigado, Colombia and from ENSAM, Paris, France in 2017. He obtained his MSc in Robotc Systems Engineering from ENSAM, Paris, France in 2018, receiving the Silver Medal honorary distinction. He is currently pursuing the PhD degree in Automatic Control at the University Paris-Saclay, France. His research interests include multi-agent systems and nonlinear control with application to autonomous robots and aerospace systems.

Antonio Loría obtained his BSc degree on Electronics Engineering from ITESM, Monterrey, Mexico in 1991 and his MSc and PhD degrees in Control Engg. from UTC, France in 1993 and 1996, respectively. He has the honour of holding a researcher position at the French National Centre of Scientific Research (CNRS) since January 1999 (Senior Researcher since 2006). He has co-authored over 250 publications on control systems and stability theory and he served as AE for *IEEE Trans. Automat. Control*, *IEEE Trans. Control Syst. Techn.*, *IEEE Control Syst. Lett.*, and the *IEEE Conf. Editorial Board*, as well as other jounrals on Automatic Control.

Dr. Ioannis Sarras (M 09) was born in Athens, Greece, in 1982. He graduated from the Automation Engineering Department of the Technological Education Institute (T.E.I.) of Piraeus, , Greece, (now University of West Attica) in 2004 and received the Master of Research (M2R) in Control Theory from the University of Paul Sabatier (France) in 2006, with scholarship from the General Michael Arnaoutis Foundation. He obtained the PhD degree with distinction in Automatic Control Systems from the university of Paris-Sud XI (France) in 2010 with a scholarship from the Greek Scholarships Foundation. From 2010 to 2017 he was a postdoctoral researcher with the Universit Libre de Bruxelles, the Laboratoire des Signaux et Systmes of the National Centre for Scientific Research (CNRS), the Department of Automatic Control of Ecole Suprieure dlectricit (SUPELEC) and the Centre of Automatic Control & Systems (CAS) of the cole Nationale Suprieure des Mines de Paris (MINES ParisTech), and ONERA-The French Aerospace Lab. During the period 2012-2013 he worked as a control engineer at the French Institute of Petroleum (IFPEn). Since 2017 he has been a Research Engineer at ONERA-The French Aerospace Lab. He has been a visiting researcher for short and long term periods at the university of Grningen, the Technical University of Catalunia, the university of Seville and the Indian Institutes of Technology in Bombay and in Madras. He has over 60 papers in peer-reviewed international journals and conferences where he has also served as a reviewer. His research activities are in the fields of nonlinear control and observer designs for single- or multi-agent systems with emphasis on aerospace applications.

Julien Marzat graduated as an engineer from ENSEM (INPL Nancy) in 2008 and completed his PhD Thesis in 2011 and Habilitation in 2019, both from University Paris-Saclay. He is currently a Research Scientist at ONERA, where his research interests include guidance, control and fault diagnosis for autonomous robots and aerospace systems.